Effects of *R*-flurbiprofen and the oxygenated metabolites of endocannabinoids in inflammatory pain mice models

Baptiste Buisseret[a], Owein Guillemot-Legris[a], Youssef Ben Kouidar[a], Adrien Paquot[a], Giulio G. Muccioli[a*], Mireille Alhouayek[a*]

a. Bioanalysis and Pharmacology of Bioactive Lipids Research Group, Louvain Drug Research Institute, Université catholique de Louvain, Avenue Mounier 72 (B1.72.01), 1200, Brussels, Belgium.

* MA and GGM share last-authorship

Mireille Alhouayek, mireille.alhouayek@uclouvain.be.

Bioanalysis and Pharmacology of Bioactive Lipids Research Group (BPBL),

Louvain Drug Research Institute (LDRI),

Université catholique de Louvain (UCL),

Av. E. Mounier, 72 (B1.72.01),

1200 Bruxelles, Belgium;

Tel: 0032 2 764 72 44

Giulio G. Muccioli, giulio.muccioli@uclouvain.be.

Bioanalysis and Pharmacology of Bioactive Lipids Research Group (BPBL),

Louvain Drug Research Institute (LDRI),

Université catholique de Louvain (UCL),

Av. E. Mounier, 72 (B1.72.01),

1200 Bruxelles, Belgium ;

Tel: 0032 2 764 72 31

Running title: Flurbiprofen enantiomers in inflammatory pain

1

ABBREVIATIONS

AEA: *N*-arachidonoylethanolamine or anandamide

2-AG: 2-arachidonoylglycerol

COX-2: cyclooxygenase-2

FAAH: fatty acid amide hydrolase

HPGDS: Hematopoietic prostaglandin D2 synthase

IL: interleukin

iNOS: inducible nitric oxide synthase

LPS: lipopolysaccharides

MAGL: monoacylglycerol lipase

mPGES1: microsomal prostaglandin E synthase 1

MPO: myeloperoxidase

NSAID: non-steroidal anti-inflammatory drugs

PG: prostaglandin

PG-EA: prostaglandin-ethanolamide

PG-G: prostaglandin-glycerol ester

SSCI: substrate-selective COX inhibitor

TNF-α: tumor necrosis factor α

ABSTRACT

Pain is one of the cardinal signs accompanying inflammation. The prostaglandins (PGs), synthetized from arachidonic acid by cyclooxygenase (COX)-2, are major bioactive lipids implicated in inflammation and pain. However, COX-2 is also able to metabolize other lipids, including the endocannabinoids 2-arachidonoylglycerol (2-AG) and anandamide (AEA), to give glycerol ester (PG-G) and ethanolamide (PG-EA) derivatives of the PGs. Consequently, COX-2 can be considered as a hub, controlling PG synthesis but also PG-G and PG-EA synthesis. As they were more recently characterized, these endocannabinoid metabolites are less studied in nociception compared to PGs. Interestingly *R*-profens, previously considered as inactive enantiomers of non-steroidal anti-inflammatory drugs (NSAIDs), are substrate-selective COX inhibitors. Indeed, *R*-flurbiprofen can selectively block PG-G and PG-EA production, without affecting PG synthesis from COX-2. Therefore, we compared the effect of *R*-flurbiprofen and *S*-flurbiprofen in models of inflammatory pain triggered by local administration of lipopolysaccharides (LPS) and carrageenan in mice. Remarkably, the effects of flurbiprofen enantiomers on mechanical hyperalgesia seem to depend on (i) the inflammatory stimuli, (ii) the route of administration and (iii) the timing of administration. We also assessed the effect of administration of the PG-Gs, PG-EAs and PGs on LPS-induced mechanical hyperalgesia. Our data support the interest of studying the non-hydrolytic endocannabinoid metabolism in the context of inflammatory pain.

KEYWORDS

Analgesia, capsaicin, eicosanoid, prostanoid, PGD_2-G, lipid mediator,

INTRODUCTION

Inflammatory pain is a common condition affecting the quality of life of many patients. A clear link between inflammation and pain has been established, along with the identification of the cells and mediators involved in initiation and maintenance of inflammatory pain. However, only few medications are currently used to tackle inflammatory pain in patients. First line treatment of acute inflammation generally relies on cyclooxygenase (COX) inhibition with non-steroidal anti-inflammatory drugs (NSAIDs). Nonetheless, side effects and lack of efficacy in chronic inflammatory processes are common limitations seen in patients [1].

Bioactive lipids are known to be key players at the interface between inflammation and pain. Among bioactive lipids, endocannabinoids and their metabolites have been put forward as new candidates to modulate both pain and the underlying inflammation [2-4]. The two major endocannabinoids, 2-arachidonoylglycerol (2-AG) and *N*-arachidonoylethanolamine (AEA or anandamide), are able to modulate nociception at multiple levels in nociceptive pathways [5]. Accordingly, administration of these lipid mediators or modulation of their metabolism are proposed as a strategy to counteract inflammatory pain [6]. The main enzymes responsible for AEA and 2-AG hydrolysis into arachidonic acid are fatty acid amide hydrolase (FAAH) and monoacylglycerol lipase (MAGL), respectively. FAAH inhibition is known to counteract inflammatory and neuropathic pain in several models [7] and MAGL inhibition is well described to counteract neuropathic, postoperative and inflammatory pain [8]. Beside their hydrolysis into arachidonic acid, oxygenation of 2-AG and AEA by COX-2 is a metabolic pathway that generates glycerol ester (PG-Gs) and ethanolamide (PG-EAs or prostamides) derivatives of the prostaglandins (PGs), respectively (Fig. S1A) [4, 9]. These prostaglandin derivatives are bioactive lipids in their own right, able to modulate inflammatory processes and pain [4, 10]. Indeed, our group demonstrated anti-inflammatory effects of the 2-AG metabolite PGD_2-G [11, 12]. We also reported that PGD_2-G counteracts inflammatory hyperalgesia in mice receiving an intra-plantar injection of carrageenan [13]. On the other hand, PGE_2-G is known to have neurotoxic, pro-inflammatory and pro-nociceptive effects [14-16]. Compared to PG-Gs, PG-EAs are less described in this context. $PGF_{2\alpha}$-EA is known to increase firing of nociceptive neurons in the dorsal horn when injected locally in the spinal cord, resulting in pro-algesic effects [17]. However, the effects of PG-EAs on peripheral nociception, a crucial process regarding inflammatory pain development, remain unknown.

Here, we hypothesized that PG-G and PG-EA production in the periphery could play a role in the development of inflammatory pain induced by various noxious stimuli. To assess this hypothesis, we administered locally or systemically a classical NSAID or substrate-selective COX inhibitor (SSCI) to modulate PG, PG-G and PG-EA production in models of inflammatory pain. Indeed, SSCIs are able to block PG-G and PG-EA production without affecting arachidonic acid metabolism and consequent PG production [18]. Thus, we selected enantiomers

of flurbiprofen for which *S*-flurbiprofen is the classical COX inhibitor and *R*-flurbiprofen is a SSCI (Fig. S1B). *R*-flurbiprofen is one of the first and better characterized SSCI and is more potent than other *R*-profens [19]. Moreover, we assessed the effect of the local administration of PGD_2, PGE_2 and $PGF_{2\alpha}$ and their corresponding glycerol ester and ethanolamide derivatives in the model of LPS-induced hyperalgesia in mice.

MATERIALS AND METHODS

Materials

R-flurbiprofen and *S*-flurbiprofen were purchased from SantaCruz Biotechnology, Inc. PGD_2, PGE_2, $PGF_{2\alpha}$, PGD_2-G, PGE_2-G, $PGF_{2\alpha}$-G, PGD_2-EA, PGE_2-EA and $PGF_{2\alpha}$-EA were from Cayman Chemicals and bought from Sanbio. Lipopolysaccharides (LPS from *E. coli*, serotype O55:B5), λ-carrageenan and capsaicin were purchased from Sigma Aldrich.

Animals

All animal care and experimental procedures were conducted in accordance with the guidelines of the local ethics committee and in accordance with European directive 2010/63/EU, which was transformed into the Belgian Law of May 29 2013 regarding the protection of laboratory animals. All experimental protocols were approved by the local ethics committee of the UCLouvain (study agreement 2017/UCL/MD/024, laboratory agreement LA1230314). Experiments were conducted using male Swiss mice (5 weeks old on arrival from Janvier Labs; 30-35 g) housed in a controlled environment with 12 hours light and dark cycle, 20-22°C temperature, 45-65% humidity, fed with a standard chow and water *ad libitum*. Prior to experimentation, all the mice were acclimatized to the animal facility for 1 week, and trained for the procedures (e.g. von Frey assessment) for an additional week. Randomization was based on arrival weight and then on paw 50% threshold after the training week for experiments requiring mechanosensitivity assessment.

Carrageenan-induced edema and hyperalgesia model

Hyperalgesia and edema were induced by λ-carrageenan injection in the plantar face of the right hind paw as described previously [13]. Briefly, 0.1 mg of λ-carrageenan or vehicle (25 µL saline) was injected in the right hind paw.

For systemic administration of the compounds, *R*-flurbiprofen (10 mg/kg), *S*-flurbiprofen (10 mg/kg) or vehicle (Saline-Tween80-DMSO, 18:1:1, v/v/v) were administered i.p. one hour after carrageenan injection and injections were then repeated at 7 hours and 13 hours after carrageenan, for a total of 3 injections per day for the duration of the study. This administration scheme was based on the reported half-life of flurbiprofen in mice [20, 21].

For intra-plantar injections, flurbiprofen enantiomers were dissolved in DMSO then diluted in saline to reach 20 µg in 20 µL of vehicle. In this setting, compounds were injected in the plantar face of the hind paw 30 minutes prior to carrageenan. Hyperalgesia and edema formation were monitored by an experimenter blinded to treatments.

Lipopolysaccharides-induced hyperalgesia model

LPS was injected in the plantar face of the right hind paw of the mice (150 ng/20 µL). The dose of LPS was chosen based on prior tests in our laboratory (Data not shown).
For systemic administration of the compounds, mice received an intra-peritoneal injection with *R*-flurbiprofen (10 mg/kg), *S*-flurbiprofen (10 mg/kg) or vehicle (Saline-Tween80-DMSO, 18:1:1, v/v/v) one hour after LPS injection and repeated at 7 hours and 13 hours after LPS, resulting in a total of 3 injections per day for the duration of the study.
For local treatments, compounds were administered 30 minutes prior to LPS in the plantar face of the hind paw of the mice. PGs, PG-Gs and PG-EAs were compared with equimolar administration, corresponding to 20 µg PGD_2-G, a dose we previously used in similar models [13]. Hyperalgesia was monitored over time by an experimenter blinded to treatments.

Capsaicin-induced nocifensive behavior

Capsaicin (1.6 µg/20 µL) or vehicle (7.5% DMSO in saline) was injected in the plantar face of the right hind paw of the mice [22]. *R*- or *S*-flurbiprofen were administered locally, 30 minutes prior to capsaicin injection. Nocifensive behavior was recorded right after capsaicin administration for 6 minutes per mouse. Then the time spent licking was measured by two independent experimenters blinded to treatments. The result is the mean, expressed in seconds, of the nocifensive behavior reported by the experimenters.

Edema monitoring

Paw thickness was measured with an electronic caliper by a blinded experimenter. For each time point, paw thickness was measured in triplicate resulting in a mean thickness. Percentage of edema formation was then calculated for each individual mouse with the following formula: $((thickness_t - thickness_{basal})/ thickness_{basal}) \times 100$, where $thickness_{basal}$ is the thickness of the paw measured prior to injections.

Hyperalgesia assessment

Von Frey's filaments were used, by a blinded experimenter, to monitor mechanical hyperalgesia as reported previously [13]. Briefly, mice were placed on a wire mesh in individual Plexiglas boxes. Prior to experiments, all animals were trained for one week for habituation to the experimental settings. After the habituation period, the

basal 50% withdrawal threshold was determined the day before the experiment with Dixon's up and down method [23] and Chaplan's calculation method [24]. A nociceptive score was calculated based on the AUC of the baseline-corrected 50% threshold monitoring [25].

Expression of inflammatory markers and enzymes measured by RT-qPCR

Paw tissue was cut, snap-frozen in liquid nitrogen and stored at -80°C prior to analysis [13]. TriPure® reagent was used to extract total RNA, following the manufacturer's instructions. cDNA was then synthetized from 1µg of RNA, by reverse transcription (RT GoScript kit, Promega). The reverse transcription cycle is composed of three steps: samples were kept for 5 minutes at 25°C then heated at 42°C for one hour and finally at 70°C during 15 minutes. Real-time qPCR analysis was performed on a QuantStudio 3 instrument (Applied Biosystems). SYBRGreen was used as intercalating dye (GoTaq qPCR Master mix, Promega) to monitor fluorescence. Sequences for the primers specific to the target genes used are reported in Table 1. A PCR run is composed of 45 cycles of amplification. Each cycle consists of three steps: 95°C for 3 seconds, 60°C for 26 seconds and 72°C for 10 seconds. At the end of the PCR reaction, melting curves of the products were realized. The 60S ribosomal protein L19 (RPL19) was used a reference gene, to normalize mRNA expression, expressed relative to control, using the "delta-delta Ct" method.

Gene / Product	Gene ref.	Product Size (bp)	Forward Primer (5' to 3')	Reverse Primer (5' to 3')
Rpl19 / RPL19	NM_009078.2 NM_001159483.1	88	TGACCTGGATGAGAAGGATGAG	CTGTGATACATATGGCGGTCAATC
Tnf / TNF-α	NM_013693.3 NM_001278601.1	94	CTACTGAACTTCGGGGTGATC	TGAGTGTGAGGGTCTGGGC
Il-6 / IL-6	NM_031168.2 NM_001314054.1	72	ACAAGTCGGAGGCTTAATTACACAT	TTGCCATTGCACAACTCTTTTC
Emr1 / F4/80	NM_010130.4 NM_001355722.1 NM_001355723.1	60	TGACAACCAGACGGCTTGTG	CAGGCGAGGAAAAGATAG
Nos2 / iNOS	NM_010927.4 NM_001313921.1 NM_001313922.1	190	AGGTACTCAGCGTGCTCCAC	GCACCGAAGATATCTTCATG
Ptgs2 / COX-2	NM_011198.4	95	TGACCCCCAAGGCTCAAATAT	TGAACCCAGGTCCTCGCTTA
Ptges / mPGES1	NM_022415.3	150	ATGAGGCTGCGGAAGAAGG	GCCGAGGAAGAGGAAAGGATAG
Hpgds / PGDS	NM_019455.4	147	TGGGAAGACAGCGTTGGAG	AGGCGAGGTGCTTGATGTG

Table 1. Primer sequences

Lipid quantification by UPLC-MS/MS

Tissue sample preparation Frozen plantar tissues were homogenized in chloroform and then internal standards (d_5-PGE_2-G, 5 pmol; d_4-PGE_2-EA, 5 pmol) were added was added to the mixture. Liquid-liquid extraction was performed by adding water and methanol, mixing thoroughly the vials and sonicating them in an iced bath during 10min. The organic layer was recovered, evaporated, suspended in organic solvent and added on solid phase extraction columns. The fraction of interest was eluted with chloroform-methanol and evaporated. The resulting fraction was solubilized in MeOH for UPLC-MS/MS analysis.

UPLC-MS/MS and data analysis Sample analysis was based on previously described methods [12, 26]. Briefly, we used a Xevo TQ-S mass spectrometer (Waters) coupled to an Acquity UPLC class H (Waters) for sample analysis. Prostaglandin separation was conducted on an Acquity UPLC BEH C18 (150 x 2.1 mm; 1.7 µm) column maintained at 40°C. Mobile phases consisted of H_2O-ACN-acetic acid (94.9:5:0.1; v/v/v) and ACN-acetic acid (99.9:0.1; v/v). A gradient was used to separate the different compounds. The mass spectrometer was employed in electrospray positive mode for compound ionisation. Multiple reaction monitoring (MRM) was used to detect and analyze the different compounds. For each, we selected one quantification (Q) transition and one qualification (q) transition that was used to confirm the peak identification. The MRM transitions determined were: 396.3→299.3 (Q) and 396.3→317.0 (q) for d_5-PGE_2-G; 391.3→299.3 (Q) and 391.3→373.2 (q) for PGE_2-G and PGD_2-G; 393.2→275.2 (Q) and 393.2→128.9 (q) for $PGF_{2\alpha}$-G; 382.2→364.3 (Q) and 382.2→346.2 (q) for d_4-PGE_2-EA; 378.2→360.2 (Q) and 378.2→342.2 (q) for PGE_2-EA and PGD_2-EA; and 380.3→344.2 (Q) and 380.3→362.2 (q) for $PGF_{2\alpha}$-EA. The MassLynx software was used for data acquisition and processing. Retention times were confirmed by analyzing pure standards of the PG-Gs and PG-EAs.

PG-EA production assay

Paw tissue from control mice was homogenized in 100 mM Tris-EDTA (TE) buffer at pH 7.4 and centrifuged at 500g for 5 min at 4°C. Supernatants were recovered and stored at -80°C until the assay was performed. Aliquots were taken for protein quantification using the DC biorad assay. PG-EA production assay was based on previously described assays for COX activity [27, 28] with some modifications. 40 µg of proteins were pre-incubated for 10 minutes at 37°C with the FAAH inhibitor PF-3845 (10 µM) to inhibit AEA hydrolysis by FAAH. d_4-AEA (10 µM) was then added to the reaction tubes and incubated for 1, 5 or 10 minutes at 37°C in TE buffer (200 µL final volume) with 0.5 mM phenol, 0.5 µM hemin and 0.5 µM reduced GSH. The reaction was stopped by addition of 0.5 mL of ice-cold MeOH on ice followed by 1mL of chloroform. The standards for UPLC-MS/MS quantification were then added and, after thorough mixing, the tubes were centrifuged at 250g for 5 min at 4°C. The organic layer was then recovered, evaporated and suspended in MeOH for UPLC-MS/MS

analysis. Potential non-biological production was assessed by incubating samples directly in the presence of methanol to denature the proteins before addition of d_4-AEA. This background was removed from the other conditions.

Cytokine quantification by ELISA

Proteins were recovered after lipid extraction and re-suspended in PBS-Triton-X100 0.05%. IL-6 and MCP-1 quantification using a sandwich-type ELISA was performed following the manufacturer's instructions (Ready-Set-Go kit from Invitrogen, ThermoFisher Scientific).

Myeloperoxidase activity assay

Myeloperoxidase (MPO) assay was performed as previously described [13]. Briefly, plantar tissue was dissected, snap frozen in liquid nitrogen and stored at -80°C. For the MPO activity assay, plantar tissues were homogenized in ice-cold 0.5% hexadecyltrimethylammonium bromide (HTAB) in 50 mM potassium phosphate buffer (pH 6), on ice. Supernatant resulting from homogenate centrifugation (20,000 x g for 20 minutes at 4°C) was recovered. Aliquots of supernatant were placed in a 96-wells microplate for the assay. 200 µL of solution containing 0.167 mg/mL *o*-dianisidine and 500 ppm hydrogen peroxide in 50 mM potassium phosphate buffer (pH 6) were then added in the 96-wells microplate. Product formation was then monitored in a spectrophotometer at 460 nm.

Statistical analysis

Data are expressed as mean ± s.e.m. Using GraphPad Prism 8 for Windows, statistical analysis was performed using one-way ANOVA or two-way ANOVA followed by Dunnett's post-hoc test. This is specified under each figure. Potential outliers were determined using Grubb's test. For clarity, significance was shown when $P<0.05$ during the time-course experiments for 50% threshold measurements of mechanical hyperalgesia and edema formation.

RESULTS

Local and systemic administration of flurbiprofen enantiomers decrease LPS-induced hyperalgesia

We first evaluated the effect of systemic administration of flurbiprofen enantiomers in the LPS-induced hyperalgesia model. Intra-plantar injection of LPS (150 ng) in mice hind paw resulted in mechanical hyperalgesia induction that lasted for 36 hours (Fig. 1A). In this setting, the dose of LPS decreased the 50% threshold, measured with von Frey's filaments, to a level where we could observe both anti- and pro-algesic effects of compounds. However, LPS did not trigger edema formation over this period of time (<5% of edema formation) (data not shown), similarly to what is observed in the literature for this model [29].
We administered treatments of *R*-flurbiprofen or *S*-flurbiprofen (10 mg/kg, i.p.) or vehicle three-times a day, starting one hour after LPS injection, throughout the study. The dose was selected based on reports studying the analgesic effects of flurbiprofen enantiomers [16, 30, 31]. *S*-flurbiprofen decreased hyperalgesia from 2 until 36 hours (Fig.1A) while *R*-flurbiprofen decreased mechanical hyperalgesia from 2 to 9 hours and from 24 to 30 hours (Fig.1A). These effects resulted in a significant decrease in the nociceptive score (Fig.1B) for both *R*- and *S*-flurbiprofen. As expected from Fig.1A, *S*-flurbiprofen was more effective than *R*-flurbiprofen to decrease the nociceptive score induced by intra-plantar injection of LPS (Fig. 1B).

Another experiment was conducted to test the effect of local administration of 20 µg *R*- or *S*-flurbiprofen in a single intra-plantar injection, 30 minutes prior to LPS administration. LPS induced hyperalgesia with a similar kinetic as previously observed. Both *S*- and *R*-flurbiprofen, given locally, decreased mechanical hyperalgesia from 2 hours until 30 and 36 hours, respectively (Fig. 1C). Interestingly, *R*-flurbiprofen decreased mechanical hyperalgesia more than *S*-flurbiprofen when administered locally in the model of LPS-induced hyperalgesia (Fig. 1C). The nociceptive score (Fig. 1D) gives a clearer overall picture of these effects.

Distinct effects of administration of flurbiprofen enantiomers on carrageenan-induced hyperalgesia

As we observed distinct effects between systemic and local administration in the LPS model of hyperalgesia, we next tested both compounds in another model, the carrageenan model of inflammation-induced hyperalgesia. Indeed, the mechanism of inflammatory pain in the carrageenan model is different from the direct TLR4 activation of the LPS model. Moreover, this model of induces a longer lasting hyperalgesia compared to LPS-induced hyperalgesia. In our settings, mechanical hyperalgesia lasted 60 hours after carrageenan administration, compared to 36 hours for LPS (Fig. 1A,C and 2A,C) [13].

Using this carrageenan-induced hyperalgesia model, we applied the same protocol for systemic treatment with enantiomers of flurbiprofen. *R*-flurbiprofen decreased mechanical hyperalgesia from 2 to 9 hours after

carrageenan injection. This anti-hyperalgesic effect of systemic *R*-flurbiprofen treatment was also observed at 24 hours and from 36 to 72 hours after carrageenan administration (Fig. 2A). Surprisingly, *S*-flurbiprofen had no effect on mechanical hyperalgesia during the first 24 hours in this model (Fig. 2A). We only noticed two time points when *S*-flurbiprofen significantly decreased hyperalgesia: 36 and 60 hours after carrageenan injection (Fig. 2A). However, when analyzing the global effect of the two compounds using the nociceptive score, we observed significant effect of both enantiomers on mechanical hyperalgesia, with the *R* enantiomer showing more effect (Fig. 2B). The same was true regarding the effect of the enantiomers on edema formation (Fig. S2).

Next, we tested the effect of local treatment with flurbiprofen enantiomers in the carrageenan-induced hyperalgesia model. With a similar administration protocol as the LPS studies, *R*-flurbiprofen decreased mechanical hyperalgesia from 2 until 30 hours after carrageenan injection (Fig. 2C). This anti-hyperalgesic effect was also significant at 48 and 60 hours following carrageenan administration. On the other hand, *S*-flurbiprofen decreased the mechanical hyperalgesia induced by carrageenan from 2 hours until 60 hours after carrageenan administration (Fig. 2C). Interestingly, we noticed that the effect of local administration of *S*-flurbiprofen was stronger in this model compared to *R*-flurbiprofen from 9 hours until 60 hours after carrageenan injection (Fig. 2C). The nociceptive score clearly shows the anti-hyperalgesic effect of both flurbiprofen enantiomers on carrageenan-induced hyperalgesia, with a stronger effect of *S*-flurbiprofen compared to *R*-flurbiprofen (Fig. 2D).

Inflammatory marker expression in the mice hind paw following LPS administration is not affected by administration of flurbiprofen enantiomers

Cytokines are known to drive the LPS-mediated hyperalgesia in the paw [32]. In light of our results, we decided to investigate further the effect of local administration of the flurbiprofen enantiomers in the LPS model, where the effect of the SSCI *R*-flurbiprofen was the strongest. To assess the effect of flurbiprofen enantiomers on inflammatory mediators, we measured cytokine expression in the paw tissue at 6 and 24 hours after LPS injection. We selected these time points as mechanical hyperalgesia is well established at 6 hours (as maintenance mechanisms are at play by immune cells) and starts to decrease at 24h. An increase in inflammatory marker expression, namely IL-6 and TNFα, was observed at 6 hours following LPS injection in the hind-paw (Fig. 3A). IL-6 protein expression followed the same induction by LPS treatment at this time point (Fig. 3B). These cytokines are known to participate in nociceptor activation and sensitization [33]. At 24 hours, cytokine expression was much lower compared to 6 hours (Fig. 3C,D), coinciding with the beginning of return to basal paw withdrawal threshold. A trend toward a decrease of IL-6 and TNFα mRNA expression was observed at 6 hours by flurbiprofen enantiomers treatments (Fig. 3A,B), while TNFα expression was

significantly higher in the paw of *S*-flurbiprofen treated mice compared to LPS-vehicle group 24 hours after LPS administration (Fig. 3C). However, both enantiomers of flurbiprofen did not affect IL-6 protein level compared to LPS-vehicle treated mice at either time point (Fig. 3B,D).

We also measured, in the paw tissue, the mRNA expression of enzymes involved in the inflammatory response and prostanoid synthesis. These include COX-2, mPGES1 (microsomal prostaglandin E synthase-1), PGDS (prostaglandin D synthase) and iNOS (inducible nitric oxide synthase). Expression of iNOS and mPGES1 were significantly increased by LPS administration at 6 hours, but not at 24h, consistent with the role of NO and PGE_2 in inflammatory hyperalgesia (Fig. 4A,B). We noted no variations of COX-2 and PGDS expression due to LPS treatment at either time point (Fig. 4A,B). At 6 hours, *R*- and *S*-flurbiprofen enantiomers decreased mPGES1 and PGDS expression compared to LPS-vehicle treated group and only *R*-flurbiprofen decreased significantly the expression of iNOS (Fig. 4A). Interestingly, COX-2 expression is increased by *R*-flurbiprofen administration at 6 hours and by *S*-flurbiprofen administration at 24 hours, compared to the LPS-vehicle group (Fig. 4A,B). Flurbiprofen enantiomers did not affect mPGES1, PGDS or iNOS expression in the hindpaw at 24 hours (Fig. 4B).

As macrophages play a crucial role in the initiation and resolution of inflammatory response and pain [34], we measured the expression of the macrophage marker F4/80 (adhesion G protein-coupled receptor E1), to assess macrophage infiltration in the paw tissue. F4/80 expression was decreased by LPS in the paw at 6 hours with a trend towards an increase at 24 hours (Fig. 4C,D). This effect is amplified by *S*-flurbiprofen at 24 hours (Fig. 4D). When activated, resident macrophages will attract neutrophils to clear the noxious stimuli at the site of injury. To assess neutrophil infiltration at 6 and 24 hours in paw tissue, we measured the myeloperoxidase (MPO) activity in the paw tissue. Indeed, MPO activity is generally considered as a marker for neutrophil presence. LPS administration did not increase MPO activity in paw tissue at 6 hours (Fig. 4E). However, this activity is increased at 24 hours following LPS injection (Fig. 4F). At both time points, MPO activity was not affected by treatments with the flurbiprofen enantiomers (Fig. 4E,F).

Administration of *R- and S-flurbiprofen enantiomers transiently delayed LPS-induced nociception recovery in mice*

Because the effect of flurbiprofen enantiomers on inflammatory hyperalgesia could not be explained by their effect on inflammation, we wanted to explore their effect at a time point where inflammation was receding but hyperalgesia was still present. Our data showed that the inflammatory tone in the paw was decreased at 24 hours compared to 6 hours following LPS intra-plantar administration (Fig. 3), although mice were still experiencing mechanical hyperalgesia at 24 hours (Fig. 1B). Therefore, we tested the effect on mechanical hyperalgesia of the local administration of flurbiprofen enantiomers 20 hours following LPS administration. As

previously observed, LPS intra-plantar injection induced a significant mechanical hyperalgesia for 36 hours. Surprisingly, when injected at 20 hours, *R*-flurbiprofen increased hyperalgesia induced by LPS at 22, 25 and 30 hours after LPS injection, compared to LPS-vehicle treated group (Fig. 5A). On the other hand, *S*-flurbiprofen did not alter hyperalgesia compared to LPS-vehicle group at 22 hours but increased hyperalgesia similarly to *R*-flurbiprofen at 25 and 30 hours following LPS administration (Fig. 5A). Therefore, administration of both flurbiprofen enantiomers led to a delay in the recovery of LPS-induced hyperalgesia. To characterize further these effects, we analyzed the nociceptive score for the recovery phase (i.e. 18 to 48 hours) of mechanical hyperalgesia kinetic. During this interval, both enantiomers significantly increased the nociceptive score compared to LPS-vehicle treated group (Fig. 5B).

R-flurbiprofen administration decreases nocifensive behavior induced by capsaicin in mice

Next, we wanted to explore the effect of flurbiprofen enantiomers on nociceptor sensitization. To this end, we used the model of hyperalgesia induced by capsaicin. Administration of capsaicin results in a strong increase of nocifensive behavior, lasting a few minutes following injection in the paw (Fig. 6A). Nocifensive behavior results from activation of TRPV1 by capsaicin at the plasma membrane of sensory neurons in the paw tissue [35]. Here we observed that *R*-flurbiprofen, but not *S*-flurbiprofen, significantly decreased the time spent by mice licking the hind paw (Fig.6A). This result suggests that *R*-flurbiprofen can directly modulate nociceptor activation, when nociceptive stimuli depend on TRPV1. In this capsaicin mouse model, neurogenic inflammation induces a secondary phase following initial sensory neuron activation, relying on substance P and CGRP release from nerve endings [36]. Mechanical hyperalgesia in this second phase was monitored at 1.5 hours after capsaicin injection (Fig. 6B). Surprisingly, *R*-flurbiprofen increased the mechanical hyperalgesia at this time, whereas *S*-flurbiprofen had no effect compared to the capsaicin-vehicle treated group (Fig. 6B).

Administration of PGs, PG-Gs and PG-EAs affect inflammatory pain induced by LPS in the paw

Because *R*-flurbiprofen and *S*-flurbiprofen had distinct effects in the paw of mice receiving LPS, we decided to study the effect of local administration of PGs and their glycerol and ethanolamide derivatives. Indeed, these lipid mediators could mediate the effects we observed with flurbiprofen enantiomers and their effect have not been previously described in the LPS-model of hyperalgesia. Based on previous experiments, we selected a dose of 20 µg of PGD_2-G and adapted the dose of other PGs, PG-Gs and PG-EAs according to their molecular weight. When comparing the effect of the D_2 series, we observed that intra-plantar administration of PGD_2-G, 30 minutes prior to LPS administration, decreased hyperalgesia induced by LPS, reaching statistical significance at 2 and 9 hours and from 24 hours until the recovery of basal hyperalgesia (Fig. 7A,B). On the other hand, PGD_2 did not affect the hyperalgesia time-course or the nociceptive score compared to LPS-vehicle treated mice, while PGD_2-EA had a slight effect on the nociceptive score (Fig.7A,B). This further supports the

notion of a beneficial effect of PGD_2-G *per se* on inflammation and hyperalgesia, as we demonstrated previously in inflammatory models [12, 13].

Another experiment was performed with the E_2 series of prostaglandin derivatives. Here also, glycerol ester and ethanolamide derivatives modulated the hyperalgesia induced by LPS. We observed that PGE_2-G increased hyperalgesia compared to LPS-vehicle treated mice from 2 hours to 36 hours after LPS injection (Fig. 7C). Conversely, PGE_2-EA showed anti-hyperalgesic properties from 5 to 24 hours and at 36 hours following LPS injection (Fig. 7C). As expected from Fig. 7C, PGE_2-G increased the nociceptive score while PGE_2-EA decreased it compared to LPS-vehicle treated mice (Fig. 7D).

Finally, in the same model, we also tested the derivatives of the F_2 series. We observed that $PGF_{2\alpha}$ and $PGF_{2\alpha}$-G significantly increased hyperalgesia compared to LPS-vehicle treated mice from 2 hours to 12 hours (Fig. 7E). This effect was also present at 30 and 36 hours after LPS injection for $PGF_{2\alpha}$ (Fig. 7E). On the other hand, $PGF_{2\alpha}$-EA showed a trend toward a decrease of hyperalgesia from 24 hours following LPS administration (Fig. 7E). Therefore, $PGF_{2\alpha}$ and $PGF_{2\alpha}$-G increased the nociceptive score while $PGF_{2\alpha}$-EA decreased the score compared to the LPS-vehicle group (Fig. 7F). Together, the data suggest an effect of these bioactive lipids in peripheral modulation of inflammatory pain induced by LPS.

As it is expected that the administration of flurbiprofen will alter PG-G and PG-EA levels, we used an UPLC-MS/MS method to assess the levels of these lipid mediators in the mouse paw following LPS and *R*- or *S*-flurbiprofen administration. Unfortunately their levels remained below the detection limit of our method, when the tissue of two paws and even four paws were used (data not shown). Nevertheless to confirm the possible production of these mediators, we incubated deuterated AEA with homogenates of paw tissues. In these conditions, d_4-PGE_2-EA is produced in a time-dependent manner (Fig. S3A). We confirmed this production using tissue homogenates from LPS-injected mice paws (Fig. S3B).

DISCUSSION

The complex system resulting from the crosstalk between endocannabinoids and prostanoids remains to be fully exploited in the context of inflammatory pain. In this intricate metabolism, COX-2 acts as a hub controlling PG, PG-G and PG-EA levels, but also potentially endocannabinoid levels [4]. Interestingly, some of the oxygenated endocannabinoid metabolites are being characterized as bioactive lipids that play a role in peripheral nociception [13, 14, 16, 17]. Here, we compared in the same setting, the effects of PGs, PG-Gs and PG-EAs on hyperalgesia induced by LPS. To our knowledge these studies are the first comparative experiments of these derivatives in parallel, allowing for a clear analysis of their effects on the time-course of mechanical hyperalgesia induced by LPS. Our data suggest that PG-EAs could counteract hyperalgesia. This work also

confirmed the previously shown anti-hyperalgesic effect of PGD_2-G [13] and pro-algesic effect of PGE_2-G [14, 16] in another model of inflammatory pain.

Furthermore, we compared substrate-selective COX inhibition (i.e. the SSCI *R*-flurbiprofen) to non-substrate-selective COX inhibition (using *S*-flurbiprofen). We observed distinct effects of *R*- and *S*-flurbiprofen that seemed to be dependent on (i) the inflammatory agent inducing hyperalgesia; (ii) the route of administration and (iii) the timing of administration. Our data show that *R*-flurbiprofen is more efficient when administered systemically in the carrageenan model of hyperalgesia and locally in the LPS model of hyperalgesia. On the other hand, *S*-flurbiprofen, a classical NSAID, is more efficient given locally in the carrageenan model and systemically in the LPS model of hyperalgesia. Regarding the carrageenan model of hyperalgesia, similar results were suggested in the literature, although mechanical hyperalgesia was not assessed [37]. Even if both the carrageenan and LPS models are models of inflammatory pain, the origin and kinetic of hyperalgesia are different and could explain part of the distinct effects of flurbiprofen enantiomers. Indeed, carrageenan appears to target macrophages and may also involve TLR2/6 receptors whereas LPS activates TLR4 receptors and signaling cascades [38, 39]. Moreover, we observed a stronger fold increase of COX-2 mRNA expression in the paw tissue following carrageenan injection compared to LPS [13].

Here, we observed that the local administration of *R*-flurbiprofen exerted the strongest anti-hyperalgesic effect in the LPS model of inflammatory pain, while *S*-flurbiprofen had minimal effects in this model. A distinct effect of these two enantiomers on inflammation in the LPS model could have explained the different effects on hyperalgesia. However, both enantiomers had little effect on paw inflammation at the time points selected. This prompted us to investigate the direct effect of both enantiomers on nociceptor activation.

As we showed in this work, *R*-flurbiprofen significantly decreased nocifensive behavior following capsaicin administration, a ligand of TRPV1 channel. TRPV1 is a ligand-gated ion channel, acting like a heat and chemical sensor on nociceptors. This channel is involved in peripheral sensitization and many inflammatory mediators can lower its activation threshold [40]. Actually it is suggested that TRPV1 activation is necessary to the initiation of carrageenan-induced mechanical hyperalgesia [41]. On the other hand, LPS is also able to sensitize TRPV1 channels, through TLR4 activation on sensory neurons [42]. Therefore, part of the anti-hyperalgesic effect of *R*-flurbiprofen could also be mediated by a decrease of TRPV1 activation in both carrageenan and LPS-induced hyperalgesia. Although, the exact mechanism of *R*-flurbiprofen on capsaicin-induced nocifensive behavior remains to be deciphered. A direct effect of flurbiprofen on TRPV1 can be fairly excluded as Rose et al. showed that it did not alter the response elicited by capsaicin in a cellular assay of TRPV1 activity [43]. Thus this effect could rely on endogenous mediators. One such mediator could be PGE_2-G.

Indeed, this lipid mediator activates $P2Y_6$ [16], which activates PKC signaling [44]. PKC in turn was shown to reduce TRPV1 activation threshold [45, 46].

Interestingly, we also noticed a pro-algesic effect of *R*-flurbiprofen, but not *S*-flurbiprofen, on mechanical hyperalgesia in capsaicin-induced neurogenic inflammation. This mechanical hyperalgesia is observed when activated sensory neurons release substance P and CGRP [47], thus further sensitizing sensory neurons [48, 49]. Therefore, *R*-flurbiprofen could impair an endogenous beneficial compensatory mechanism in this model. This mechanism could be also at play during the recovery from LPS-induced mechanical hyperalgesia. In this case, both flurbiprofen enantiomers delayed the recovery from mechanical hyperalgesia when injected at 20 hours after LPS intra-plantar injection. Because *R*-flurbiprofen prevented hyperalgesia when given prior to LPS, we could hypothesize that a detrimental pathway is blocked by *R*-flurbiprofen, potentially involving PGE_2-G and $PGF_{2\alpha}$-G. Indeed, we showed that these metabolites are detrimental in the LPS-induced hyperalgesia model. This pathway could be changing during the recovery phase of hyperalgesia and can switch towards the synthesis of beneficial metabolites (e.g. PGD_2-G). Supporting this notion, a change in the production of pro-inflammatory to pro-resolutive metabolites of COX-2 was also previously described for PG synthesis, depending on the phase of the inflammatory reaction [50]. In agreement with a deleterious effect of *R*-flurbiprofen in some settings, previous work in the lab showed that *R*-flurbiprofen prevented PGD_2-G production following increased 2-AG levels in LPS-activated macrophages and blocked the beneficial effects observed with inhibition of 2-AG hydrolysis in these cells [11]. While we were able to show ex vivo production of PG-EAs in paw tissue homogenates, the quantification of oxygenated endocannabinoid metabolites remains elusive in vivo. Further studies are warranted to investigate the kinetics of PG-G and PG-EA formation during inflammatory pain and whether they are involved in the effects of flurbiprofen enantiomers on inflammatory pain.

Moreover, part of the beneficial effect of *R*-flurbiprofen could be due to substrates (i.e. 2-AG and AEA) because they are known to counteract hyperalgesia [51]. Indeed, by inhibiting COX-2-mediated oxygenation of the endocannabinoids, *R*-flurbiprofen could lead to increased 2-AG and AEA levels. Moreover, both flurbiprofen enantiomers were shown to be weak inhibitors of FAAH [52] and could therefore increase AEA levels. Moreover, some effects of flurbirpofen enantiomers were attributed to CB_1 and/or CB_2 receptor activation [31, 53]. Whether this is due to COX-2 or FAAH remains to be explored.

Moreover, it was suggested that some effects of *R*-flurbiprofen could be due to its bioconversion into *S*-flurbiprofen. However, we can fairly exclude the relevance of α-methylacyl-CoA racemase-dependent bioconversion of *R*-flurbiprofen into *S*-flurbiprofen [54] as the two enantiomers had, for the most part, different effects. Indeed, when given locally, strong distinct effects where observed and maintained over time for

flurbiprofen enantiomers, suggesting low bioconversion in the paw tissue. Distinct effects were also observed for systemic administration, weakening the bioconversion hypothesis. Besides the potential involvement of oxygenated metabolites of endocannabinoids and the potential bioconversion of *R*-flurbiprofen into *S*-flurbiprofen, we cannot exclude an effect unrelated to COX inhibition in the effects of flurbiprofen enantiomers.

In conclusion, *R*-flurbiprofen showed anti-hyperalgesic properties in mice receiving LPS or carrageenan in the paw. However, our data suggest that the crosstalk between the endocannabinoids and prostanoids in inflammatory pain is difficult to fine tune to achieve analgesia. Moreover, COX-2 shows a complex kinetic, depending on multiple parameters, suggesting that its complete blockade does not appear to be the best solution in all settings. Our data indicate that depending on the type of nociceptive stimuli, the treatment strategy could change. Moreover, we showed that PG-Gs and PG-EAs are bioactive lipids that can modulate nociception in the LPS model of hyperalgesia. However, their exact role and effectors during the initiation and maintenance of inflammatory hyperalgesia remain to be elucidated. Nevertheless, these results underline the interest of deciphering the exact mechanism of action of both inflammatory stimuli and treatments. Indeed, depending on the origin of inflammatory pain, treatment choice and route of administration could be adapted.

Authors' contributions

B. Buisseret, M. Alhouayek and G.G. Muccioli designed research; B. Buisseret, A. Paquot, M. Alhouayek, Y. Ben Kouidar, O. Guillemot-legris and G.G. Muccioli performed experiments and analyzed data; B. Buisseret, M. Alhouayek and G.G. Muccioli wrote the paper. All authors read and approved the manuscript.

Acknowledgments :

O.G.-L. and M.A. are postdoctoral researchers from the FRS-FNRS (Fonds de la Recherche Scientifique) Belgium. G.G.M. is the recipient of subsidies from the Fonds Spéciaux de Recherches (FSR, Université catholique de Louvain) and from the FRS-FNRS, Belgium.

Conflict of interest statement:

The authors have no competing interests to declare

References

1. Sala, A.; Proschak, E.; Steinhilber, D.; Rovati, G. E., Two-pronged approach to anti-inflammatory therapy through the modulation of the arachidonic acid cascade. *Biochem Pharmacol* **2018,** *158*, 161-173.
2. Piomelli, D.; Hohmann, A. G.; Seybold, V.; Hammock, B. D., A lipid gate for the peripheral control of pain. *J Neurosci* **2014,** *34* (46), 15184-91.
3. Donvito, G.; Nass, S. R.; Wilkerson, J. L.; Curry, Z. A.; Schurman, L. D.; Kinsey, S. G.; Lichtman, A. H., The Endogenous Cannabinoid System: A Budding Source of Targets for Treating Inflammatory and Neuropathic Pain. *Neuropsychopharmacology* **2018,** *43* (1), 52-79.
4. Buisseret, B.; Alhouayek, M.; Guillemot-Legris, O.; Muccioli, G. G., Endocannabinoid and Prostanoid Crosstalk in Pain. *Trends Mol Med* **2019,** *25* (10), 882-896.
5. Woodhams, S. G.; Chapman, V.; Finn, D. P.; Hohmann, A. G.; Neugebauer, V., The cannabinoid system and pain. *Neuropharmacology* **2017,** *124*, 105-120.
6. Guindon, J.; Hohmann, A. G., The endocannabinoid system and pain. *CNS Neurol Disord Drug Targets* **2009,** *8* (6), 403-21.
7. Sasso, O.; Wagner, K.; Morisseau, C.; Inceoglu, B.; Hammock, B. D.; Piomelli, D., Peripheral FAAH and soluble epoxide hydrolase inhibitors are synergistically antinociceptive. *Pharmacol Res* **2015,** *97*, 7-15.
8. Clapper, J. R.; Henry, C. L.; Niphakis, M. J.; Knize, A. M.; Coppola, A. R.; Simon, G. M.; Ngo, N.; Herbst, R. A.; Herbst, D. M.; Reed, A. W.; Cisar, J. S.; Weber, O. D.; Viader, A.; Alexander, J. P.; Cunningham, M. L.; Jones, T. K.; Fraser, I. P.; Grice, C. A.; Ezekowitz, R. A. B.; O'Neill, G. P.; Blankman, J. L., Monoacylglycerol Lipase Inhibition in Human and Rodent Systems Supports Clinical Evaluation of Endocannabinoid Modulators. *J Pharmacol Exp Ther* **2018,** *367* (3), 494-508.
9. Kozak, K. R.; Crews, B. C.; Morrow, J. D.; Wang, L. H.; Ma, Y. H.; Weinander, R.; Jakobsson, P. J.; Marnett, L. J., Metabolism of the endocannabinoids, 2-arachidonylglycerol and anandamide, into prostaglandin, thromboxane, and prostacyclin glycerol esters and ethanolamides. *J Biol Chem* **2002,** *277* (47), 44877-85.
10. Alhouayek, M.; Muccioli, G. G., COX-2-derived endocannabinoid metabolites as novel inflammatory mediators. *Trends Pharmacol Sci* **2014,** *35* (6), 284-92.
11. Alhouayek, M.; Masquelier, J.; Cani, P. D.; Lambert, D. M.; Muccioli, G. G., Implication of the anti-inflammatory bioactive lipid prostaglandin D2-glycerol ester in the control of macrophage activation and inflammation by ABHD6. *Proc Natl Acad Sci U S A* **2013,** *110* (43), 17558-63.
12. Alhouayek, M.; Buisseret, B.; Paquot, A.; Guillemot-Legris, O.; Muccioli, G. G., The endogenous bioactive lipid prostaglandin D2-glycerol ester reduces murine colitis via DP1 and PPARgamma receptors. *FASEB J* **2018,** *32* (9), 5000-5011.
13. Buisseret, B.; Guillemot-Legris, O.; Muccioli, G. G.; Alhouayek, M., Prostaglandin D2-glycerol ester decreases carrageenan-induced inflammation and hyperalgesia in mice. *Biochim Biophys Acta Mol Cell Biol Lipids* **2019,** *1864* (5), 609-618.
14. Hu, S. S.; Bradshaw, H. B.; Chen, J. S.; Tan, B.; Walker, J. M., Prostaglandin E2 glycerol ester, an endogenous COX-2 metabolite of 2-arachidonoylglycerol, induces hyperalgesia and modulates NFkappaB activity. *Br J Pharmacol* **2008,** *153* (7), 1538-49.
15. Valdeolivas, S.; Pazos, M. R.; Bisogno, T.; Piscitelli, F.; Iannotti, F. A.; Allara, M.; Sagredo, O.; Di Marzo, V.; Fernandez-Ruiz, J., The inhibition of 2-arachidonoyl-glycerol (2-AG) biosynthesis, rather than enhancing striatal damage, protects striatal neurons from malonate-induced death: a potential role of cyclooxygenase-2-dependent metabolism of 2-AG. *Cell Death Dis* **2013,** *4*, e862.
16. Khasabova, I. A.; Uhelski, M.; Khasabov, S. G.; Gupta, K.; Seybold, V. S.; Simone, D. A., Sensitization of nociceptors by prostaglandin E2-glycerol contributes to hyperalgesia in mice with sickle cell disease. *Blood* **2019,** *133* (18), 1989-1998.
17. Gatta, L.; Piscitelli, F.; Giordano, C.; Boccella, S.; Lichtman, A.; Maione, S.; Di Marzo, V., Discovery of prostamide F2alpha and its role in inflammatory pain and dorsal horn nociceptive neuron hyperexcitability. *PLoS One* **2012,** *7* (2), e31111.
18. Hermanson, D. J.; Gamble-George, J. C.; Marnett, L. J.; Patel, S., Substrate-selective COX-2 inhibition as a novel strategy for therapeutic endocannabinoid augmentation. *Trends Pharmacol Sci* **2014,** *35* (7), 358-67.

19. Duggan, K. C.; Hermanson, D. J.; Musee, J.; Prusakiewicz, J. J.; Scheib, J. L.; Carter, B. D.; Banerjee, S.; Oates, J. A.; Marnett, L. J., (R)-Profens are substrate-selective inhibitors of endocannabinoid oxygenation by COX-2. *Nat Chem Biol* **2011,** *7* (11), 803-9.
20. Leipold, D. D.; Kantoci, D.; Murray, E. D., Jr.; Quiggle, D. D.; Wechter, W. J., Bioinversion of R-flurbiprofen to S-flurbiprofen at various dose levels in rat, mouse, and monkey. *Chirality* **2004,** *16* (6), 379-87.
21. Jamali, F.; Berry, B. W.; Tehrani, M. R.; Russell, A. S., Stereoselective pharmacokinetics of flurbiprofen in humans and rats. *J Pharm Sci* **1988,** *77* (8), 666-9.
22. Sakurada, T.; Katsumata, K.; Tan-No, K.; Sakurada, S.; Kisara, K., The capsaicin test in mice for evaluating tachykinin antagonists in the spinal cord. *Neuropharmacology* **1992,** *31* (12), 1279-85.
23. Dixon, W. J., Efficient analysis of experimental observations. *Annu Rev Pharmacol Toxicol* **1980,** *20*, 441-62.
24. Chaplan, S. R.; Bach, F. W.; Pogrel, J. W.; Chung, J. M.; Yaksh, T. L., Quantitative assessment of tactile allodynia in the rat paw. *J Neurosci Methods* **1994,** *53* (1), 55-63.
25. Edwards, S. R.; Mather, L. E.; Smith, M. T., Studies with ketamine and alfentanil following Freund's complete adjuvant-induced inflammation in rats. *Clin Exp Pharmacol Physiol* **2007,** *34* (5-6), 414-20.
26. Bottemanne, P.; Paquot, A.; Ameraoui, H.; Alhouayek, M.; Muccioli, G. G., The alpha/beta-hydrolase domain 6 inhibitor WWL70 decreases endotoxin-induced lung inflammation in mice, potential contribution of 2-arachidonoylglycerol, and lysoglycerophospholipids. *FASEB J* **2019,** *33* (6), 7635-7646.
27. Ayoub, S. S., In vitro cyclooxygenase activity assay in tissue homogenates. *Methods Mol Biol* **2010,** *644*, 117-20.
28. Kalgutkar, A. S.; Marnett, L. J., Rapid inactivation of prostaglandin endoperoxide synthases by N-(carboxyalkyl)maleimides. *Biochemistry* **1994,** *33* (29), 8625-8.
29. Booker, L.; Kinsey, S. G.; Abdullah, R. A.; Blankman, J. L.; Long, J. Z.; Ezzili, C.; Boger, D. L.; Cravatt, B. F.; Lichtman, A. H., The fatty acid amide hydrolase (FAAH) inhibitor PF-3845 acts in the nervous system to reverse LPS-induced tactile allodynia in mice. *Br J Pharmacol* **2012,** *165* (8), 2485-96.
30. Neugebauer, V.; Geisslinger, G.; Rumenapp, P.; Weiretter, F.; Szelenyi, I.; Brune, K.; Schaible, H. G., Antinociceptive effects of R(-)- and S(+)-flurbiprofen on rat spinal dorsal horn neurons rendered hyperexcitable by an acute knee joint inflammation. *J Pharmacol Exp Ther* **1995,** *275* (2), 618-28.
31. Bishay, P.; Schmidt, H.; Marian, C.; Haussler, A.; Wijnvoord, N.; Ziebell, S.; Metzner, J.; Koch, M.; Myrczek, T.; Bechmann, I.; Kuner, R.; Costigan, M.; Dehghani, F.; Geisslinger, G.; Tegeder, I., R-flurbiprofen reduces neuropathic pain in rodents by restoring endogenous cannabinoids. *PLoS One* **2010,** *5* (5), e10628.
32. Calil, I. L.; Zarpelon, A. C.; Guerrero, A. T.; Alves-Filho, J. C.; Ferreira, S. H.; Cunha, F. Q.; Cunha, T. M.; Verri, W. A., Jr., Lipopolysaccharide induces inflammatory hyperalgesia triggering a TLR4/MyD88-dependent cytokine cascade in the mice paw. *PLoS One* **2014,** *9* (3), e90013.
33. Sommer, C.; Kress, M., Recent findings on how proinflammatory cytokines cause pain: peripheral mechanisms in inflammatory and neuropathic hyperalgesia. *Neurosci Lett* **2004,** *361* (1-3), 184-7.
34. Bang, S.; Xie, Y. K.; Zhang, Z. J.; Wang, Z.; Xu, Z. Z.; Ji, R. R., GPR37 regulates macrophage phagocytosis and resolution of inflammatory pain. *J Clin Invest* **2018,** *128* (8), 3568-3582.
35. Yang, F.; Zheng, J., Understand spiciness: mechanism of TRPV1 channel activation by capsaicin. *Protein Cell* **2017,** *8* (3), 169-177.
36. Matsuda, M.; Huh, Y.; Ji, R. R., Roles of inflammation, neurogenic inflammation, and neuroinflammation in pain. *J Anesth* **2019,** *33* (1), 131-139.
37. Buritova, J.; Besson, J. M., Peripheral and/or central effects of racemic-, S(+)- and R(-)-flurbiprofen on inflammatory nociceptive processes: a c-Fos protein study in the rat spinal cord. *Br J Pharmacol* **1998,** *125* (1), 87-101.
38. Catanzaro, P. J.; Schwartz, H. J.; Graham, R. C., Jr., Spectrum and possible mechanism of carrageenan cytotoxicity. *Am J Pathol* **1971,** *64* (2), 387-404.
39. Myers, M. J.; Deaver, C. M.; Lewandowski, A. J., Molecular mechanism of action responsible for carrageenan-induced inflammatory response. *Mol Immunol* **2019,** *109*, 38-42.
40. Bennett, D. L.; Clark, A. J.; Huang, J.; Waxman, S. G.; Dib-Hajj, S. D., The Role of Voltage-Gated Sodium Channels in Pain Signaling. *Physiol Rev* **2019,** *99* (2), 1079-1151.
41. Watanabe, M.; Ueda, T.; Shibata, Y.; Kumamoto, N.; Ugawa, S., The role of TRPV1 channels in carrageenan-induced mechanical hyperalgesia in mice. *Neuroreport* **2015,** *26* (3), 173-8.

42. Diogenes, A.; Ferraz, C. C.; Akopian, A. N.; Henry, M. A.; Hargreaves, K. M., LPS sensitizes TRPV1 via activation of TLR4 in trigeminal sensory neurons. *J Dent Res* **2011,** *90* (6), 759-64.
43. Rose, T. M.; Reilly, C. A.; Deering-Rice, C. E.; Brewster, C.; Brewster, C., Inhibition of FAAH, TRPV1, and COX2 by NSAID-serotonin conjugates. *Bioorg Med Chem Lett* **2014,** *24* (24), 5695-5698.
44. Kim, S. G.; Gao, Z. G.; Soltysiak, K. A.; Chang, T. S.; Brodie, C.; Jacobson, K. A., P2Y6 nucleotide receptor activates PKC to protect 1321N1 astrocytoma cells against tumor necrosis factor-induced apoptosis. *Cell Mol Neurobiol* **2003,** *23* (3), 401-18.
45. Numazaki, M.; Tominaga, T.; Toyooka, H.; Tominaga, M., Direct phosphorylation of capsaicin receptor VR1 by protein kinase Cepsilon and identification of two target serine residues. *J Biol Chem* **2002,** *277* (16), 13375-8.
46. Vellani, V.; Mapplebeck, S.; Moriondo, A.; Davis, J. B.; McNaughton, P. A., Protein kinase C activation potentiates gating of the vanilloid receptor VR1 by capsaicin, protons, heat and anandamide. *J Physiol* **2001,** *534* (Pt 3), 813-25.
47. Chiu, I. M.; von Hehn, C. A.; Woolf, C. J., Neurogenic inflammation and the peripheral nervous system in host defense and immunopathology. *Nat Neurosci* **2012,** *15* (8), 1063-7.
48. Ansel, J. C.; Brown, J. R.; Payan, D. G.; Brown, M. A., Substance P selectively activates TNF-alpha gene expression in murine mast cells. *J Immunol* **1993,** *150* (10), 4478-85.
49. Mikami, N.; Matsushita, H.; Kato, T.; Kawasaki, R.; Sawazaki, T.; Kishimoto, T.; Ogitani, Y.; Watanabe, K.; Miyagi, Y.; Sueda, K.; Fukada, S.; Yamamoto, H.; Tsujikawa, K., Calcitonin gene-related peptide is an important regulator of cutaneous immunity: effect on dendritic cell and T cell functions. *J Immunol* **2011,** *186* (12), 6886-93.
50. Gilroy, D. W.; Colville-Nash, P. R.; Willis, D.; Chivers, J.; Paul-Clark, M. J.; Willoughby, D. A., Inducible cyclooxygenase may have anti-inflammatory properties. *Nat Med* **1999,** *5* (6), 698-701.
51. Woodhams, S. G.; Sagar, D. R.; Burston, J. J.; Chapman, V., The role of the endocannabinoid system in pain. *Handb Exp Pharmacol* **2015,** *227*, 119-43.
52. Fowler, C. J.; Janson, U.; Johnson, R. M.; Wahlstrom, G.; Stenstrom, A.; Norstrom, K.; Tiger, G., Inhibition of anandamide hydrolysis by the enantiomers of ibuprofen, ketorolac, and flurbiprofen. *Arch Biochem Biophys* **1999,** *362* (2), 191-6.
53. Ates, M.; Hamza, M.; Seidel, K.; Kotalla, C. E.; Ledent, C.; Guhring, H., Intrathecally applied flurbiprofen produces an endocannabinoid-dependent antinociception in the rat formalin test. *Eur J Neurosci* **2003,** *17* (3), 597-604.
54. de Bruin, N.; Ferreiros, N.; Schmidt, M.; Hofmann, M.; Angioni, C.; Geisslinger, G.; Parnham, M. J., Mutual inversion of flurbiprofen enantiomers in various rat and mouse strains. *Chirality* **2018,** *30* (5), 632-641.

Figure legends

Fig. 1. Systemic or local administration of flurbiprofen enantiomers decrease LPS-induced hyperalgesia.

Mice received, in 20 µL, 150 ng of LPS or saline by intra-plantar injection in the right hind paw. Mechanical hyperalgesia was monitored by an experimenter blinded to treatments using von Frey's filaments for 54 hours after LPS injection. **(A, B)** Enantiomers of flurbiprofen were administered intra-peritoneally 3 times a day. (A) Time course of mechanical hyperalgesia. The horizontal dashed line represents the mean basal 50% threshold of all groups. (B) The nociceptive score (g*h) is the basal corrected area under the curve (AUC) from the data in A. **(C, D)** Enantiomers of flurbiprofen were administered locally 30 minutes prior to LPS administration in the paw. (C) Time-course of mechanical hyperalgesia. The horizontal dashed line represents the mean basal 50% threshold of all groups. (D) The nociceptive score (g*h) is the basal corrected AUC from the data in C. Values are presented as mean ± s.e.m., n=8 animals per group. For hyperalgesia monitoring graphs (A and C): *P < 0.05 compared to the vehicle-treated LPS group, $ P < 0.05 for *S*-flurbiprofen compared to *R*-flurbiprofen treated groups, using two-way ANOVA and Holm-Sidak's multiple comparison post-hoc test. For histograms (B and D): ** P < 0.01, *** P < 0.001, compared to vehicle-treated LPS group, $$ *P* < 0.01, $$$ P < 0.001 for *S*-flurbiprofen compared to *R*-flurbiprofen treated groups, using one-way ANOVA and Dunnett's post-hoc test.

Fig. 2. Systemic or local administration of flurbiprofen enantiomers affect carrageenan-induced hyperalgesia.

Hyperalgesia was induced in mice by injection of 0.1 mg in 25 µL of carrageenan in the plantar face of the right hind paw. Mechanical hyperalgesia was monitored by an experimenter blinded to treatments using von Frey's filaments for 80 hours after carrageenan injection. **(A, B)** Enantiomers of flurbiprofen were administered intra-peritoneally 3 times a day. (A) Time course of mechanical hyperalgesia. The horizontal dashed line represents the mean basal 50% threshold of all groups. (B) The nociceptive score (g*h) is the basal corrected area under the curve (AUC) from the data in A. **(C, D)** Enantiomers of flurbiprofen were administered locally 30 minutes prior to carrageenan administration in the paw. (C) Time-course of mechanical hyperalgesia. The horizontal dashed line represents the mean basal 50% threshold of all groups. (D) The nociceptive score (g*h) is the basal corrected AUC from the data in C. Values are presented as mean ± s.e.m., n=8 animals per group. For hyperalgesia monitoring graphs (A and C): *P < 0.05, ** *P* < 0.01 compared to vehicle-treated carrageenan group, $ P < 0.05 for *S*-flurbiprofen compared to *R*-flurbiprofen treated groups, using two-way ANOVA and Holm-Sidak's multiple comparison post-hoc test. For histograms (B and D): * P < 0.05, *** P < 0.001

compared to the vehicle-treated carrageenan group, $ P < 0.05 for *S*-flurbiprofen compared to *R*-flurbiprofen treated groups using one-way ANOVA and Dunnett's post-hoc test.

Fig. 3. Expression of inflammatory cytokines in the paw of mice treated with LPS and vehicle or flurbiprofen enantiomers.

Mice received, in 20 µL, 150 ng of LPS or saline by intra-plantar injection in the right hind paw. Local injections of flurbiprofen enantiomers or vehicle were carried out 30 minutes prior to LPS injection. **(A)** mRNA expression of IL-6 and TNFα in the mice plantar tissue at 6 hours following LPS administration, measured by RT-qPCR. **(B)** IL-6 protein levels in the paw tissue measured by ELISA, at 6 hours after LPS injection. **(C)** mRNA expression of IL-6 and TNFα in the mice plantar tissue at 24 hours following LPS administration, measured by RT-qPCR. **(D)** IL-6 protein levels in the paw tissue measured by ELISA at 24 hours following LPS injection. mRNA expression is expressed relative to the control group (Veh. without LPS) set at 1. Values are presented as mean ± s.e.m., n=8 animals per group. *P < 0.05, ** P < 0.01, *** P < 0.001, compared to the vehicle-treated LPS group, using one-way ANOVA and Dunnett's post-hoc test.

Fig. 4. Expression of enzymes and immune cell markers in the paw of mice treated with and vehicle or flurbiprofen enantiomers.

Mice received, in 20 µL, 150 ng of LPS or saline by intra-plantar injection in the right hind paw. Local injections of flurbiprofen enantiomers or vehicle were carried out 30 minutes prior to LPS injection. **(A,B)** mRNA expression of COX-2, iNOS, mPGES1 and PGDS in the plantar tissue at (A) 6 hours or (B) 24 hours following LPS administration, measured by RT-qPCR. **(C, D)** mRNA expression of the pan-macrophage marker F4/80 in the plantar tissue at (C) 6 hours or (D) 24 hours following LPS administration, measured by RT-qPCR. **(E, F)** MPO activity measured in the plantar tissue at (E) 6 hours or (F) 24 hours following LPS administration. mRNA expression is expressed relative to the control group (Veh. without LPS) set at 1. Values are presented as mean ± s.e.m., n=8 animals per group. * P < 0.05, ** P < 0.01, *** P < 0.001, compared to the vehicle-treated LPS group, $ P<0.05, $$$ P<0.001, for *S*-flurbiprofen compared to *R*-flurbiprofen treated groups, using one-way ANOVA and Dunnett's post-hoc test.

Fig. 5. Local administration of flurbiprofen enantiomers at 20 hours post intra-plantar LPS worsens hyperalgesia.

Mice received, in 20 µL, 150 ng of LPS or saline by intra-plantar injection in the right hind paw. Flurbiprofen enantiomers were administered locally 20 hours after LPS administration. (A) Time-course of mechanical hyperalgesia development was monitored by a blinded experimenter using von Frey's filaments. The mean basal 50% threshold of all groups is represented by horizontal dashed line. (B) The nociceptive score (g*h) based on the area under the curve from 18 to 48 hours post LPS injection. Values are presented as mean ± s.e.m., n=8 animals per group. * $P < 0.05$, ** $P < 0.01$ *** $P < 0.001$, compared to the vehicle-treated LPS group, using two-way ANOVA for A or one-way ANOVA for B followed by Dunnett's post-hoc test.

Fig. 6. Effect of flurbiprofen enantiomers on capsaicin-induced hyperalgesia model.

Hyperalgesia was induced by intra-plantar injection of 1.6 µg of capsaicin triggering nocifensive behavior and mechanical hyperalgesia. **(A)** Nocifensive behavior is recorded for 5 minutes and measured by blinded experimenters. **(B)** Paw withdrawal threshold is determined at 1.5 hours after capsaicin injection. Values are presented as mean ± s.e.m., n=8 animals per group. * $P < 0.05$, ** $P < 0.01$, *** $P < 0.001$, compared to the vehicle-treated LPS group, using two-way ANOVA for A or one-way ANOVA for B followed by Dunnett's post-hoc test.

Fig. 7. Intra-plantar administration of prostaglandins, prostaglandin glycerol esters and prostamides affects LPS-induced hyperalgesia.

Mice received, in 20 µL, 150 ng of LPS or saline by intra-plantar injection in the right hind paw. Local injections of PG, PG-Gs, PG-EAs or vehicle were carried out 30 minutes prior to LPS injections. Mechanical hyperalgesia was monitored by an experimenter blinded to treatments using von Frey's filaments for 54 hours after LPS injection. **(A, C, E)** Time course of mechanical hyperalgesia. The horizontal dashed line represents the mean basal 50% threshold of all groups. **(B, D, F)** The nociceptive score (g*h) is the basal corrected area under the curve from the data in A, C or E, respectively. Values are presented as mean ± s.e.m., n=8 animals per group. For hyperalgesia monitoring graphs (A, C, E): * $P < 0.05$ compared to the vehicle-treated LPS group, using two-way ANOVA and Dunnett's multiple comparison post-hoc test. For histograms (B, D, F): * $P < 0.05$, ** $P < 0.01$, *** $P < 0.001$, compared to vehicle-treated LPS group, using one-way ANOVA and Dunnett's post-hoc test.

Effects of *R*-flurbiprofen and the oxygenated metabolites of endocannabinoids in inflammatory pain mice models

Baptiste Buisseret[a], Owein Guillemot-Legris[a], Youssef Ben Kouidar[a], Adrien Paquot[a], Giulio G. Muccioli[a*], Mireille Alhouayek[a*]

a. Bioanalysis and Pharmacology of Bioactive Lipids Research Group, Louvain Drug Research Institute, Université catholique de Louvain, Avenue Mounier 72 (B1.72.01), 1200, Brussels, Belgium.

* MA and GGM share last-authorship

Mireille Alhouayek, mireille.alhouayek@uclouvain.be.

Bioanalysis and Pharmacology of Bioactive Lipids Research Group (BPBL),

Louvain Drug Research Institute (LDRI),

Université catholique de Louvain (UCL),

Av. E. Mounier, 72 (B1.72.01),

1200 Bruxelles, Belgium;

Tel: 0032 2 764 72 44

Giulio G. Muccioli, giulio.muccioli@uclouvain.be.

Bioanalysis and Pharmacology of Bioactive Lipids Research Group (BPBL),

Louvain Drug Research Institute (LDRI),

Université catholique de Louvain (UCL),

Av. E. Mounier, 72 (B1.72.01),

1200 Bruxelles, Belgium ;

Tel: 0032 2 764 72 31

Running title: Flurbiprofen enantiomers in inflammatory pain

1

ABBREVIATIONS

AEA: *N*-arachidonoylethanolamine or anandamide

2-AG: 2-arachidonoylglycerol

COX-2: cyclooxygenase-2

FAAH: fatty acid amide hydrolase

HPGDS: Hematopoietic prostaglandin D2 synthase

IL: interleukin

iNOS: inducible nitric oxide synthase

LPS: lipopolysaccharides

MAGL: monoacylglycerol lipase

mPGES1: microsomal prostaglandin E synthase 1

MPO: myeloperoxidase

NSAID: non-steroidal anti-inflammatory drugs

PG: prostaglandin

PG-EA: prostaglandin-ethanolamide

PG-G: prostaglandin-glycerol ester

SSCI: substrate-selective COX inhibitor

TNF-α: tumor necrosis factor α

ABSTRACT

Pain is one of the cardinal signs accompanying inflammation. The prostaglandins (PGs), synthetized from arachidonic acid by cyclooxygenase (COX)-2, are major bioactive lipids implicated in inflammation and pain. However, COX-2 is also able to metabolize other lipids, including the endocannabinoids 2-arachidonoylglycerol (2-AG) and anandamide (AEA), to give glycerol ester (PG-G) and ethanolamide (PG-EA) derivatives of the PGs. Consequently, COX-2 can be considered as a hub, controlling PG synthesis but also PG-G and PG-EA synthesis. As they were more recently characterized, these endocannabinoid metabolites are less studied in nociception compared to PGs. Interestingly *R*-profens, previously considered as inactive enantiomers of non-steroidal anti-inflammatory drugs (NSAIDs), are substrate-selective COX inhibitors. Indeed, *R*-flurbiprofen can selectively block PG-G and PG-EA production, without affecting PG synthesis from COX-2. Therefore, we compared the effect of *R*-flurbiprofen and *S*-flurbiprofen in models of inflammatory pain triggered by local administration of lipopolysaccharides (LPS) and carrageenan in mice. Remarkably, the effects of flurbiprofen enantiomers on mechanical hyperalgesia seem to depend on (i) the inflammatory stimuli, (ii) the route of administration and (iii) the timing of administration. We also assessed the effect of administration of the PG-Gs, PG-EAs and PGs on LPS-induced mechanical hyperalgesia. Our data support the interest of studying the non-hydrolytic endocannabinoid metabolism in the context of inflammatory pain.

KEYWORDS

Analgesia, capsaicin, eicosanoid, prostanoid, PGD_2-G, lipid mediator,

INTRODUCTION

Inflammatory pain is a common condition affecting the quality of life of many patients. A clear link between inflammation and pain has been established, along with the identification of the cells and mediators involved in initiation and maintenance of inflammatory pain. However, only few medications are currently used to tackle inflammatory pain in patients. First line treatment of acute inflammation generally relies on cyclooxygenase (COX) inhibition with non-steroidal anti-inflammatory drugs (NSAIDs). Nonetheless, side effects and lack of efficacy in chronic inflammatory processes are common limitations seen in patients [1].

Bioactive lipids are known to be key players at the interface between inflammation and pain. Among bioactive lipids, endocannabinoids and their metabolites have been put forward as new candidates to modulate both pain and the underlying inflammation [2-4]. The two major endocannabinoids, 2-arachidonoylglycerol (2-AG) and *N*-arachidonoylethanolamine (AEA or anandamide), are able to modulate nociception at multiple levels in nociceptive pathways [5]. Accordingly, administration of these lipid mediators or modulation of their metabolism are proposed as a strategy to counteract inflammatory pain [6]. The main enzymes responsible for AEA and 2-AG hydrolysis into arachidonic acid are fatty acid amide hydrolase (FAAH) and monoacylglycerol lipase (MAGL), respectively. FAAH inhibition is known to counteract inflammatory and neuropathic pain in several models [7] and MAGL inhibition is well described to counteract neuropathic, postoperative and inflammatory pain [8]. Beside their hydrolysis into arachidonic acid, oxygenation of 2-AG and AEA by COX-2 is a metabolic pathway that generates glycerol ester (PG-Gs) and ethanolamide (PG-EAs or prostamides) derivatives of the prostaglandins (PGs), respectively (Fig. S1A) [4, 9]. These prostaglandin derivatives are bioactive lipids in their own right, able to modulate inflammatory processes and pain [4, 10]. Indeed, our group demonstrated anti-inflammatory effects of the 2-AG metabolite PGD_2-G [11, 12]. We also reported that PGD_2-G counteracts inflammatory hyperalgesia in mice receiving an intra-plantar injection of carrageenan [13]. On the other hand, PGE_2-G is known to have neurotoxic, pro-inflammatory and pro-nociceptive effects [14-16]. Compared to PG-Gs, PG-EAs are less described in this context. $PGF_{2\alpha}$-EA is known to increase firing of nociceptive neurons in the dorsal horn when injected locally in the spinal cord, resulting in pro-algesic effects [17]. However, the effects of PG-EAs on peripheral nociception, a crucial process regarding inflammatory pain development, remain unknown.

Here, we hypothesized that PG-G and PG-EA production in the periphery could play a role in the development of inflammatory pain induced by various noxious stimuli. To assess this hypothesis, we administered locally or systemically a classical NSAID or substrate-selective COX inhibitor (SSCI) to modulate PG, PG-G and PG-EA production in models of inflammatory pain. Indeed, SSCIs are able to block PG-G and PG-EA production without affecting arachidonic acid metabolism and consequent PG production [18]. Thus, we selected enantiomers

of flurbiprofen for which *S*-flurbiprofen is the classical COX inhibitor and *R*-flurbiprofen is a SSCI (Fig. S1B). *R*-flurbiprofen is one of the first and better characterized SSCI and is more potent than other *R*-profens [19]. Moreover, we assessed the effect of the local administration of PGD_2, PGE_2 and $PGF_{2\alpha}$ and their corresponding glycerol ester and ethanolamide derivatives in the model of LPS-induced hyperalgesia in mice.

MATERIALS AND METHODS

Materials

R-flurbiprofen and *S*-flurbiprofen were purchased from SantaCruz Biotechnology, Inc. PGD_2, PGE_2, $PGF_{2\alpha}$, PGD_2-G, PGE_2-G, $PGF_{2\alpha}$-G, PGD_2-EA, PGE_2-EA and $PGF_{2\alpha}$-EA were from Cayman Chemicals and bought from Sanbio. Lipopolysaccharides (LPS from *E. coli*, serotype O55:B5), λ-carrageenan and capsaicin were purchased from Sigma Aldrich.

Animals

All animal care and experimental procedures were conducted in accordance with the guidelines of the local ethics committee and in accordance with European directive 2010/63/EU, which was transformed into the Belgian Law of May 29 2013 regarding the protection of laboratory animals. All experimental protocols were approved by the local ethics committee of the UCLouvain (study agreement 2017/UCL/MD/024, laboratory agreement LA1230314). Experiments were conducted using male Swiss mice (5 weeks old on arrival from Janvier Labs; 30-35 g) housed in a controlled environment with 12 hours light and dark cycle, 20-22°C temperature, 45-65% humidity, fed with a standard chow and water *ad libitum*. Prior to experimentation, all the mice were acclimatized to the animal facility for 1 week, and trained for the procedures (e.g. von Frey assessment) for an additional week. Randomization was based on arrival weight and then on paw 50% threshold after the training week for experiments requiring mechanosensitivity assessment.

Carrageenan-induced edema and hyperalgesia model

Hyperalgesia and edema were induced by λ-carrageenan injection in the plantar face of the right hind paw as described previously [13]. Briefly, 0.1 mg of λ-carrageenan or vehicle (25 µL saline) was injected in the right hind paw.

For systemic administration of the compounds, *R*-flurbiprofen (10 mg/kg), *S*-flurbiprofen (10 mg/kg) or vehicle (Saline-Tween80-DMSO, 18:1:1, v/v/v) were administered i.p. one hour after carrageenan injection and injections were then repeated at 7 hours and 13 hours after carrageenan, for a total of 3 injections per day for the duration of the study. This administration scheme was based on the reported half-life of flurbiprofen in mice [20, 21].

For intra-plantar injections, flurbiprofen enantiomers were dissolved in DMSO then diluted in saline to reach 20 µg in 20 µL of vehicle. In this setting, compounds were injected in the plantar face of the hind paw 30 minutes prior to carrageenan. Hyperalgesia and edema formation were monitored by an experimenter blinded to treatments.

Lipopolysaccharides-induced hyperalgesia model

LPS was injected in the plantar face of the right hind paw of the mice (150 ng/20 µL). The dose of LPS was chosen based on prior tests in our laboratory (Data not shown).
For systemic administration of the compounds, mice received an intra-peritoneal injection with *R*-flurbiprofen (10 mg/kg), *S*-flurbiprofen (10 mg/kg) or vehicle (Saline-Tween80-DMSO, 18:1:1, v/v/v) one hour after LPS injection and repeated at 7 hours and 13 hours after LPS, resulting in a total of 3 injections per day for the duration of the study.
For local treatments, compounds were administered 30 minutes prior to LPS in the plantar face of the hind paw of the mice. PGs, PG-Gs and PG-EAs were compared with equimolar administration, corresponding to 20 µg PGD_2-G, a dose we previously used in similar models [13]. Hyperalgesia was monitored over time by an experimenter blinded to treatments.

Capsaicin-induced nocifensive behavior

Capsaicin (1.6 µg/20 µL) or vehicle (7.5% DMSO in saline) was injected in the plantar face of the right hind paw of the mice [22]. *R*- or *S*-flurbiprofen were administered locally, 30 minutes prior to capsaicin injection. Nocifensive behavior was recorded right after capsaicin administration for 6 minutes per mouse. Then the time spent licking was measured by two independent experimenters blinded to treatments. The result is the mean, expressed in seconds, of the nocifensive behavior reported by the experimenters.

Edema monitoring

Paw thickness was measured with an electronic caliper by a blinded experimenter. For each time point, paw thickness was measured in triplicate resulting in a mean thickness. Percentage of edema formation was then calculated for each individual mouse with the following formula: $((thickness_t - thickness_{basal})/ thickness_{basal}) \times 100$, where $thickness_{basal}$ is the thickness of the paw measured prior to injections.

Hyperalgesia assessment

Von Frey's filaments were used, by a blinded experimenter, to monitor mechanical hyperalgesia as reported previously [13]. Briefly, mice were placed on a wire mesh in individual Plexiglas boxes. Prior to experiments, all animals were trained for one week for habituation to the experimental settings. After the habituation period, the

basal 50% withdrawal threshold was determined the day before the experiment with Dixon's up and down method [23] and Chaplan's calculation method [24]. A nociceptive score was calculated based on the AUC of the baseline-corrected 50% threshold monitoring [25].

Expression of inflammatory markers and enzymes measured by RT-qPCR

Paw tissue was cut, snap-frozen in liquid nitrogen and stored at -80°C prior to analysis [13]. TriPure® reagent was used to extract total RNA, following the manufacturer's instructions. cDNA was then synthetized from 1µg of RNA, by reverse transcription (RT GoScript kit, Promega). The reverse transcription cycle is composed of three steps: samples were kept for 5 minutes at 25°C then heated at 42°C for one hour and finally at 70°C during 15 minutes. Real-time qPCR analysis was performed on a QuantStudio 3 instrument (Applied Biosystems). SYBRGreen was used as intercalating dye (GoTaq qPCR Master mix, Promega) to monitor fluorescence. Sequences for the primers specific to the target genes used are reported in Table 1. A PCR run is composed of 45 cycles of amplification. Each cycle consists of three steps: 95°C for 3 seconds, 60°C for 26 seconds and 72°C for 10 seconds. At the end of the PCR reaction, melting curves of the products were realized. The 60S ribosomal protein L19 (RPL19) was used a reference gene, to normalize mRNA expression, expressed relative to control, using the "delta-delta Ct" method.

Gene / Product	Gene ref.	Product Size (bp)	Forward Primer (5' to 3')	Reverse Primer (5' to 3')
Rpl19 / RPL19	NM_009078.2 NM_001159483.1	88	TGACCTGGATGAGAAGGATGAG	CTGTGATACATATGGCGGTCAATC
Tnf / TNF-α	NM_013693.3 NM_001278601.1	94	CTACTGAACTTCGGGGTGATC	TGAGTGTGAGGGTCTGGGC
Il-6 / IL-6	NM_031168.2 NM_001314054.1	72	ACAAGTCGGAGGCTTAATTACACAT	TTGCCATTGCACAACTCTTTTC
Emr1 / F4/80	NM_010130.4 NM_001355722.1 NM_001355723.1	60	TGACAACCAGACGGCTTGTG	CAGGCGAGGAAAAGATAG
Nos2 / iNOS	NM_010927.4 NM_001313921.1 NM_001313922.1	190	AGGTACTCAGCGTGCTCCAC	GCACCGAAGATATCTTCATG
Ptgs2 / COX-2	NM_011198.4	95	TGACCCCCAAGGCTCAAATAT	TGAACCCAGGTCCTCGCTTA
Ptges / mPGES1	NM_022415.3	150	ATGAGGCTGCGGAAGAAGG	GCCGAGGAAGAGGAAAGGATAG
Hpgds / PGDS	NM_019455.4	147	TGGGAAGACAGCGTTGGAG	AGGCGAGGTGCTTGATGTG

Table 1. Primer sequences

Lipid quantification by UPLC-MS/MS

Tissue sample preparation Frozen plantar tissues were homogenized in chloroform and then internal standards (d_5-PGE_2-G, 5 pmol; d_4-PGE_2-EA, 5 pmol) were added was added to the mixture. Liquid-liquid extraction was performed by adding water and methanol, mixing thoroughly the vials and sonicating them in an iced bath during 10min. The organic layer was recovered, evaporated, suspended in organic solvent and added on solid phase extraction columns. The fraction of interest was eluted with chloroform-methanol and evaporated. The resulting fraction was solubilized in MeOH for UPLC-MS/MS analysis.

UPLC-MS/MS and data analysis Sample analysis was based on previously described methods [12, 26]. Briefly, we used a Xevo TQ-S mass spectrometer (Waters) coupled to an Acquity UPLC class H (Waters) for sample analysis. Prostaglandin separation was conducted on an Acquity UPLC BEH C18 (150 x 2.1 mm; 1.7 µm) column maintained at 40°C. Mobile phases consisted of H_2O-ACN-acetic acid (94.9:5:0.1; v/v/v) and ACN-acetic acid (99.9:0.1; v/v). A gradient was used to separate the different compounds. The mass spectrometer was employed in electrospray positive mode for compound ionisation. Multiple reaction monitoring (MRM) was used to detect and analyze the different compounds. For each, we selected one quantification (Q) transition and one qualification (q) transition that was used to confirm the peak identification. The MRM transitions determined were: 396.3→299.3 (Q) and 396.3→317.0 (q) for d_5-PGE_2-G; 391.3→299.3 (Q) and 391.3→373.2 (q) for PGE_2-G and PGD_2-G; 393.2→275.2 (Q) and 393.2→128.9 (q) for $PGF_{2\alpha}$-G; 382.2→364.3 (Q) and 382.2→346.2 (q) for d_4-PGE_2-EA; 378.2→360.2 (Q) and 378.2→342.2 (q) for PGE_2-EA and PGD_2-EA; and 380.3→344.2 (Q) and 380.3→362.2 (q) for $PGF_{2\alpha}$-EA. The MassLynx software was used for data acquisition and processing. Retention times were confirmed by analyzing pure standards of the PG-Gs and PG-EAs.

PG-EA production assay

Paw tissue from control mice was homogenized in 100 mM Tris-EDTA (TE) buffer at pH 7.4 and centrifuged at 500g for 5 min at 4°C. Supernatants were recovered and stored at -80°C until the assay was performed. Aliquots were taken for protein quantification using the DC biorad assay. PG-EA production assay was based on previously described assays for COX activity [27, 28] with some modifications. 40 µg of proteins were pre-incubated for 10 minutes at 37°C with the FAAH inhibitor PF-3845 (10 µM) to inhibit AEA hydrolysis by FAAH. d_4-AEA (10 µM) was then added to the reaction tubes and incubated for 1, 5 or 10 minutes at 37°C in TE buffer (200 µL final volume) with 0.5 mM phenol, 0.5 µM hemin and 0.5 µM reduced GSH. The reaction was stopped by addition of 0.5 mL of ice-cold MeOH on ice followed by 1mL of chloroform. The standards for UPLC-MS/MS quantification were then added and, after thorough mixing, the tubes were centrifuged at 250g for 5 min at 4°C. The organic layer was then recovered, evaporated and suspended in MeOH for UPLC-MS/MS

analysis. Potential non-biological production was assessed by incubating samples directly in the presence of methanol to denature the proteins before addition of d_4-AEA. This background was removed from the other conditions.

Cytokine quantification by ELISA

Proteins were recovered after lipid extraction and re-suspended in PBS-Triton-X100 0.05%. IL-6 and MCP-1 quantification using a sandwich-type ELISA was performed following the manufacturer's instructions (Ready-Set-Go kit from Invitrogen, ThermoFisher Scientific).

Myeloperoxidase activity assay

Myeloperoxidase (MPO) assay was performed as previously described [13]. Briefly, plantar tissue was dissected, snap frozen in liquid nitrogen and stored at -80°C. For the MPO activity assay, plantar tissues were homogenized in ice-cold 0.5% hexadecyltrimethylammonium bromide (HTAB) in 50 mM potassium phosphate buffer (pH 6), on ice. Supernatant resulting from homogenate centrifugation (20,000 x g for 20 minutes at 4°C) was recovered. Aliquots of supernatant were placed in a 96-wells microplate for the assay. 200 µL of solution containing 0.167 mg/mL *o*-dianisidine and 500 ppm hydrogen peroxide in 50 mM potassium phosphate buffer (pH 6) were then added in the 96-wells microplate. Product formation was then monitored in a spectrophotometer at 460 nm.

Statistical analysis

Data are expressed as mean ± s.e.m. Using GraphPad Prism 8 for Windows, statistical analysis was performed using one-way ANOVA or two-way ANOVA followed by Dunnett's post-hoc test. This is specified under each figure. Potential outliers were determined using Grubb's test. For clarity, significance was shown when $P<0.05$ during the time-course experiments for 50% threshold measurements of mechanical hyperalgesia and edema formation.

RESULTS

Local and systemic administration of flurbiprofen enantiomers decrease LPS-induced hyperalgesia

We first evaluated the effect of systemic administration of flurbiprofen enantiomers in the LPS-induced hyperalgesia model. Intra-plantar injection of LPS (150 ng) in mice hind paw resulted in mechanical hyperalgesia induction that lasted for 36 hours (Fig. 1A). In this setting, the dose of LPS decreased the 50% threshold, measured with von Frey's filaments, to a level where we could observe both anti- and pro-algesic effects of compounds. However, LPS did not trigger edema formation over this period of time (<5% of edema formation) (data not shown), similarly to what is observed in the literature for this model [29].
We administered treatments of *R*-flurbiprofen or *S*-flurbiprofen (10 mg/kg, i.p.) or vehicle three-times a day, starting one hour after LPS injection, throughout the study. The dose was selected based on reports studying the analgesic effects of flurbiprofen enantiomers [16, 30, 31]. *S*-flurbiprofen decreased hyperalgesia from 2 until 36 hours (Fig.1A) while *R*-flurbiprofen decreased mechanical hyperalgesia from 2 to 9 hours and from 24 to 30 hours (Fig.1A). These effects resulted in a significant decrease in the nociceptive score (Fig.1B) for both *R*- and *S*-flurbiprofen. As expected from Fig.1A, *S*-flurbiprofen was more effective than *R*-flurbiprofen to decrease the nociceptive score induced by intra-plantar injection of LPS (Fig. 1B).

Another experiment was conducted to test the effect of local administration of 20 µg *R*- or *S*-flurbiprofen in a single intra-plantar injection, 30 minutes prior to LPS administration. LPS induced hyperalgesia with a similar kinetic as previously observed. Both *S*- and *R*-flurbiprofen, given locally, decreased mechanical hyperalgesia from 2 hours until 30 and 36 hours, respectively (Fig. 1C). Interestingly, *R*-flurbiprofen decreased mechanical hyperalgesia more than *S*-flurbiprofen when administered locally in the model of LPS-induced hyperalgesia (Fig. 1C). The nociceptive score (Fig. 1D) gives a clearer overall picture of these effects.

Distinct effects of administration of flurbiprofen enantiomers on carrageenan-induced hyperalgesia

As we observed distinct effects between systemic and local administration in the LPS model of hyperalgesia, we next tested both compounds in another model, the carrageenan model of inflammation-induced hyperalgesia. Indeed, the mechanism of inflammatory pain in the carrageenan model is different from the direct TLR4 activation of the LPS model. Moreover, this model of induces a longer lasting hyperalgesia compared to LPS-induced hyperalgesia. In our settings, mechanical hyperalgesia lasted 60 hours after carrageenan administration, compared to 36 hours for LPS (Fig. 1A,C and 2A,C) [13].

Using this carrageenan-induced hyperalgesia model, we applied the same protocol for systemic treatment with enantiomers of flurbiprofen. *R*-flurbiprofen decreased mechanical hyperalgesia from 2 to 9 hours after

carrageenan injection. This anti-hyperalgesic effect of systemic *R*-flurbiprofen treatment was also observed at 24 hours and from 36 to 72 hours after carrageenan administration (Fig. 2A). Surprisingly, *S*-flurbiprofen had no effect on mechanical hyperalgesia during the first 24 hours in this model (Fig. 2A). We only noticed two time points when *S*-flurbiprofen significantly decreased hyperalgesia: 36 and 60 hours after carrageenan injection (Fig. 2A). However, when analyzing the global effect of the two compounds using the nociceptive score, we observed significant effect of both enantiomers on mechanical hyperalgesia, with the *R* enantiomer showing more effect (Fig. 2B). The same was true regarding the effect of the enantiomers on edema formation (Fig. S2).

Next, we tested the effect of local treatment with flurbiprofen enantiomers in the carrageenan-induced hyperalgesia model. With a similar administration protocol as the LPS studies, *R*-flurbiprofen decreased mechanical hyperalgesia from 2 until 30 hours after carrageenan injection (Fig. 2C). This anti-hyperalgesic effect was also significant at 48 and 60 hours following carrageenan administration. On the other hand, *S*-flurbiprofen decreased the mechanical hyperalgesia induced by carrageenan from 2 hours until 60 hours after carrageenan administration (Fig. 2C). Interestingly, we noticed that the effect of local administration of *S*-flurbiprofen was stronger in this model compared to *R*-flurbiprofen from 9 hours until 60 hours after carrageenan injection (Fig. 2C). The nociceptive score clearly shows the anti-hyperalgesic effect of both flurbiprofen enantiomers on carrageenan-induced hyperalgesia, with a stronger effect of *S*-flurbiprofen compared to *R*-flurbiprofen (Fig. 2D).

Inflammatory marker expression in the mice hind paw following LPS administration is not affected by administration of flurbiprofen enantiomers

Cytokines are known to drive the LPS-mediated hyperalgesia in the paw [32]. In light of our results, we decided to investigate further the effect of local administration of the flurbiprofen enantiomers in the LPS model, where the effect of the SSCI *R*-flurbiprofen was the strongest. To assess the effect of flurbiprofen enantiomers on inflammatory mediators, we measured cytokine expression in the paw tissue at 6 and 24 hours after LPS injection. We selected these time points as mechanical hyperalgesia is well established at 6 hours (as maintenance mechanisms are at play by immune cells) and starts to decrease at 24h. An increase in inflammatory marker expression, namely IL-6 and TNFα, was observed at 6 hours following LPS injection in the hind-paw (Fig. 3A). IL-6 protein expression followed the same induction by LPS treatment at this time point (Fig. 3B). These cytokines are known to participate in nociceptor activation and sensitization [33]. At 24 hours, cytokine expression was much lower compared to 6 hours (Fig. 3C,D), coinciding with the beginning of return to basal paw withdrawal threshold. A trend toward a decrease of IL-6 and TNFα mRNA expression was observed at 6 hours by flurbiprofen enantiomers treatments (Fig. 3A,B), while TNFα expression was

significantly higher in the paw of *S*-flurbiprofen treated mice compared to LPS-vehicle group 24 hours after LPS administration (Fig. 3C). However, both enantiomers of flurbiprofen did not affect IL-6 protein level compared to LPS-vehicle treated mice at either time point (Fig. 3B,D).

We also measured, in the paw tissue, the mRNA expression of enzymes involved in the inflammatory response and prostanoid synthesis. These include COX-2, mPGES1 (microsomal prostaglandin E synthase-1), PGDS (prostaglandin D synthase) and iNOS (inducible nitric oxide synthase). Expression of iNOS and mPGES1 were significantly increased by LPS administration at 6 hours, but not at 24h, consistent with the role of NO and PGE_2 in inflammatory hyperalgesia (Fig. 4A,B). We noted no variations of COX-2 and PGDS expression due to LPS treatment at either time point (Fig. 4A,B). At 6 hours, *R*- and *S*-flurbiprofen enantiomers decreased mPGES1 and PGDS expression compared to LPS-vehicle treated group and only *R*-flurbiprofen decreased significantly the expression of iNOS (Fig. 4A). Interestingly, COX-2 expression is increased by *R*-flurbiprofen administration at 6 hours and by *S*-flurbiprofen administration at 24 hours, compared to the LPS-vehicle group (Fig. 4A,B). Flurbiprofen enantiomers did not affect mPGES1, PGDS or iNOS expression in the hindpaw at 24 hours (Fig. 4B).

As macrophages play a crucial role in the initiation and resolution of inflammatory response and pain [34], we measured the expression of the macrophage marker F4/80 (adhesion G protein-coupled receptor E1), to assess macrophage infiltration in the paw tissue. F4/80 expression was decreased by LPS in the paw at 6 hours with a trend towards an increase at 24 hours (Fig. 4C,D). This effect is amplified by *S*-flurbiprofen at 24 hours (Fig. 4D). When activated, resident macrophages will attract neutrophils to clear the noxious stimuli at the site of injury. To assess neutrophil infiltration at 6 and 24 hours in paw tissue, we measured the myeloperoxidase (MPO) activity in the paw tissue. Indeed, MPO activity is generally considered as a marker for neutrophil presence. LPS administration did not increase MPO activity in paw tissue at 6 hours (Fig. 4E). However, this activity is increased at 24 hours following LPS injection (Fig. 4F). At both time points, MPO activity was not affected by treatments with the flurbiprofen enantiomers (Fig. 4E,F).

Administration of *R- and S-flurbiprofen enantiomers transiently delayed LPS-induced nociception recovery in mice*

Because the effect of flurbiprofen enantiomers on inflammatory hyperalgesia could not be explained by their effect on inflammation, we wanted to explore their effect at a time point where inflammation was receding but hyperalgesia was still present. Our data showed that the inflammatory tone in the paw was decreased at 24 hours compared to 6 hours following LPS intra-plantar administration (Fig. 3), although mice were still experiencing mechanical hyperalgesia at 24 hours (Fig. 1B). Therefore, we tested the effect on mechanical hyperalgesia of the local administration of flurbiprofen enantiomers 20 hours following LPS administration. As

previously observed, LPS intra-plantar injection induced a significant mechanical hyperalgesia for 36 hours. Surprisingly, when injected at 20 hours, *R*-flurbiprofen increased hyperalgesia induced by LPS at 22, 25 and 30 hours after LPS injection, compared to LPS-vehicle treated group (Fig. 5A). On the other hand, *S*-flurbiprofen did not alter hyperalgesia compared to LPS-vehicle group at 22 hours but increased hyperalgesia similarly to *R*-flurbiprofen at 25 and 30 hours following LPS administration (Fig. 5A). Therefore, administration of both flurbiprofen enantiomers led to a delay in the recovery of LPS-induced hyperalgesia. To characterize further these effects, we analyzed the nociceptive score for the recovery phase (i.e. 18 to 48 hours) of mechanical hyperalgesia kinetic. During this interval, both enantiomers significantly increased the nociceptive score compared to LPS-vehicle treated group (Fig. 5B).

R-flurbiprofen administration decreases nocifensive behavior induced by capsaicin in mice

Next, we wanted to explore the effect of flurbiprofen enantiomers on nociceptor sensitization. To this end, we used the model of hyperalgesia induced by capsaicin. Administration of capsaicin results in a strong increase of nocifensive behavior, lasting a few minutes following injection in the paw (Fig. 6A). Nocifensive behavior results from activation of TRPV1 by capsaicin at the plasma membrane of sensory neurons in the paw tissue [35]. Here we observed that *R*-flurbiprofen, but not *S*-flurbiprofen, significantly decreased the time spent by mice licking the hind paw (Fig.6A). This result suggests that *R*-flurbiprofen can directly modulate nociceptor activation, when nociceptive stimuli depend on TRPV1. In this capsaicin mouse model, neurogenic inflammation induces a secondary phase following initial sensory neuron activation, relying on substance P and CGRP release from nerve endings [36]. Mechanical hyperalgesia in this second phase was monitored at 1.5 hours after capsaicin injection (Fig. 6B). Surprisingly, *R*-flurbiprofen increased the mechanical hyperalgesia at this time, whereas *S*-flurbiprofen had no effect compared to the capsaicin-vehicle treated group (Fig. 6B).

Administration of PGs, PG-Gs and PG-EAs affect inflammatory pain induced by LPS in the paw

~~As it is expected that the administration of *R*-flurbiprofen will alter PG-G and PG-EA levels, we used an LC-MS/MS method to assess the levels of these lipid mediators in the mouse paw following LPS and *R*- or *S*-flurbiprofen administration. Unfortunately their levels remained below the detection limit of our method, even when the tissue of two paws were used.~~

Because *R*-flurbiprofen and *S*-flurbiprofen had distinct effects in the paw of mice receiving LPS, we decided to study the effect of local administration of PGs and their glycerol and ethanolamide derivatives. Indeed, these lipid mediators could mediate the effects we observed with flurbiprofen enantiomers and their effect have not been previously described in the LPS-model of hyperalgesia. Based on previous experiments, we selected a dose of 20 µg of PGD_2-G and adapted the dose of other PGs, PG-Gs and PG-EAs according to their molecular

weight. When comparing the effect of the D_2 series, we observed that intra-plantar administration of PGD_2-G, 30 minutes prior to LPS administration, decreased hyperalgesia induced by LPS, reaching statistical significance at 2 and 9 hours and from 24 hours until the recovery of basal hyperalgesia (Fig. 7A,B). On the other hand, PGD_2 did not affect the hyperalgesia time-course or the nociceptive score compared to LPS-vehicle treated mice, while PGD_2-EA had a slight effect on the nociceptive score (Fig.7A,B). This further supports the notion of a beneficial effect of PGD_2-G *per se* on inflammation and hyperalgesia, as we demonstrated previously in inflammatory models [12, 13].

Another experiment was performed with the E_2 series of prostaglandin derivatives. Here also, glycerol ester and ethanolamide derivatives modulated the hyperalgesia induced by LPS. We observed that PGE_2-G increased hyperalgesia compared to LPS-vehicle treated mice from 2 hours to 36 hours after LPS injection (Fig. 7C). Conversely, PGE_2-EA showed anti-hyperalgesic properties from 5 to 24 hours and at 36 hours following LPS injection (Fig. 7C). As expected from Fig. 7C, PGE_2-G increased the nociceptive score while PGE_2-EA decreased it compared to LPS-vehicle treated mice (Fig. 7D).

Finally, in the same model, we also tested the derivatives of the F_2 series. We observed that $PGF_{2\alpha}$ and $PGF_{2\alpha}$-G significantly increased hyperalgesia compared to LPS-vehicle treated mice from 2 hours to 12 hours (Fig. 7E). This effect was also present at 30 and 36 hours after LPS injection for $PGF_{2\alpha}$ (Fig. 7E). On the other hand, $PGF_{2\alpha}$-EA showed a trend toward a decrease of hyperalgesia from 24 hours following LPS administration (Fig. 7E). Therefore, $PGF_{2\alpha}$ and $PGF_{2\alpha}$-G increased the nociceptive score while $PGF_{2\alpha}$-EA decreased the score compared to the LPS-vehicle group (Fig. 7F). Together, the data suggest an effect of these bioactive lipids in peripheral modulation of inflammatory pain induced by LPS.

As it is expected that the administration of flurbiprofen will alter PG-G and PG-EA levels, we used an UPLC-MS/MS method to assess the levels of these lipid mediators in the mouse paw following LPS and *R*- or *S*-flurbiprofen administration. Unfortunately their levels remained below the detection limit of our method, when the tissue of two paws and even four paws were used (data not shown). Nevertheless to confirm the possible production of these mediators, we incubated deuterated AEA with homogenates of paw tissues. In these conditions, d_4-PGE_2-EA is produced in a time-dependent manner (Fig. S3A). We confirmed this production using tissue homogenates from LPS-injected mice paws (Fig. S3B).

DISCUSSION

The complex system resulting from the crosstalk between endocannabinoids and prostanoids remains to be fully exploited in the context of inflammatory pain. In this intricate metabolism, COX-2 acts as a hub controlling PG, PG-G and PG-EA levels, but also potentially endocannabinoid levels [4]. Interestingly, some of

the oxygenated endocannabinoid metabolites are being characterized as bioactive lipids that play a role in peripheral nociception [13, 14, 16, 17]. Here, we compared in the same setting, the effects of PGs, PG-Gs and PG-EAs on hyperalgesia induced by LPS. To our knowledge these studies are the first comparative experiments of these derivatives in parallel, allowing for a clear analysis of their effects on the time-course of mechanical hyperalgesia induced by LPS. Our data suggest that PG-EAs could counteract hyperalgesia. This work also confirmed the previously shown anti-hyperalgesic effect of PGD_2-G [13] and pro-algesic effect of PGE_2-G [14, 16] in another model of inflammatory pain.

Furthermore, we compared substrate-selective COX inhibition (i.e. the SSCI *R*-flurbiprofen) to non-substrate-selective COX inhibition (using *S*-flurbiprofen). We observed distinct effects of *R*- and *S*-flurbiprofen that seemed to be dependent on (i) the inflammatory agent inducing hyperalgesia; (ii) the route of administration and (iii) the timing of administration. Our data show that *R*-flurbiprofen is more efficient when administered systemically in the carrageenan model of hyperalgesia and locally in the LPS model of hyperalgesia. On the other hand, *S*-flurbiprofen, a classical NSAID, is more efficient given locally in the carrageenan model and systemically in the LPS model of hyperalgesia. Regarding the carrageenan model of hyperalgesia, similar results were suggested in the literature, although mechanical hyperalgesia was not assessed [37]. Even if both the carrageenan and LPS models are models of inflammatory pain, the origin and kinetic of hyperalgesia are different and could explain part of the distinct effects of flurbiprofen enantiomers. Indeed, carrageenan appears to target macrophages and may also involve TLR2/6 receptors whereas LPS activates TLR4 receptors and signaling cascades [38, 39]. Moreover, we observed a stronger fold increase of COX-2 mRNA expression in the paw tissue following carrageenan injection compared to LPS [13].

Here, we observed that the local administration of *R*-flurbiprofen exerted the strongest anti-hyperalgesic effect in the LPS model of inflammatory pain, while *S*-flurbiprofen had minimal effects in this model. A distinct effect of these two enantiomers on inflammation in the LPS model could have explained the different effects on hyperalgesia. However, both enantiomers had little effect on paw inflammation at the time points selected. This prompted us to investigate the direct effect of both enantiomers on nociceptor activation.

As we showed in this work, *R*-flurbiprofen significantly decreased nocifensive behavior following capsaicin administration, a ligand of TRPV1 channel. TRPV1 is a ligand-gated ion channel, acting like a heat and chemical sensor on nociceptors. This channel is involved in peripheral sensitization and many inflammatory mediators can lower its activation threshold [40]. Actually it is suggested that TRPV1 activation is necessary to the initiation of carrageenan-induced mechanical hyperalgesia [41]. On the other hand, LPS is also able to sensitize TRPV1 channels, through TLR4 activation on sensory neurons [42]. Therefore, part of the anti-hyperalgesic effect of *R*-flurbiprofen could also be mediated by a decrease of TRPV1 activation in both

carrageenan and LPS-induced hyperalgesia. Although, the exact mechanism of *R*-flurbiprofen on capsaicin-induced nocifensive behavior remains to be deciphered. A direct effect of flurbiprofen on TRPV1 can be fairly excluded as Rose et al. showed that it did not alter the response elicited by capsaicin in a cellular assay of TRPV1 activity [43]. Thus this effect could rely on endogenous mediators. One such mediator could be PGE_2-G. Indeed, this lipid mediator activates $P2Y_6$ [16], which activates PKC signaling [44]. PKC in turn was shown to reduce TRPV1 activation threshold [45, 46].

Interestingly, we also noticed a pro-algesic effect of *R*-flurbiprofen, but not *S*-flurbiprofen, on mechanical hyperalgesia in capsaicin-induced neurogenic inflammation. This mechanical hyperalgesia is observed when activated sensory neurons release substance P and CGRP [47], thus further sensitizing sensory neurons [48, 49]. Therefore, *R*-flurbiprofen could impair an endogenous beneficial compensatory mechanism in this model. This mechanism could be also at play during the recovery from LPS-induced mechanical hyperalgesia. In this case, both flurbiprofen enantiomers delayed the recovery from mechanical hyperalgesia when injected at 20 hours after LPS intra-plantar injection. Because *R*-flurbiprofen prevented hyperalgesia when given prior to LPS, we could hypothesize that a detrimental pathway is blocked by *R*-flurbiprofen, potentially involving PGE_2-G and $PGF_{2\alpha}$-G. Indeed, we showed that these metabolites are detrimental in the LPS-induced hyperalgesia model. This pathway could be changing during the recovery phase of hyperalgesia and can switch towards the synthesis of beneficial metabolites (e.g. PGD_2-G). Supporting this notion, a change in the production of pro-inflammatory to pro-resolutive metabolites of COX-2 was also previously described for PG synthesis, depending on the phase of the inflammatory reaction [50]. In agreement with a deleterious effect of *R*-flurbiprofen in some settings, previous work in the lab showed that *R*-flurbiprofen prevented PGD_2-G production following increased 2-AG levels in LPS-activated macrophages and blocked the beneficial effects observed with inhibition of 2-AG hydrolysis in these cells [11]. While we were able to show ex vivo production of PG-EAs in paw tissue homogenates, the quantification of oxygenated endocannabinoid metabolites remains elusive in vivo. Further studies are warranted to investigate the kinetics of PG-G and PG-EA formation during inflammatory pain and whether they are involved in the effects of flurbiprofen enantiomers on inflammatory pain.

Moreover, part of the beneficial effect of *R*-flurbiprofen could be due to substrates (i.e. 2-AG and AEA) because they are known to counteract hyperalgesia [51]. Indeed, by inhibiting COX-2-mediated oxygenation of the endocannabinoids, *R*-flurbiprofen could lead to increased 2-AG and AEA levels. Moreover, both flurbiprofen enantiomers were shown to be weak inhibitors of FAAH [52] and could therefore increase AEA levels. Moreover, some effects of flurbirpofen enantiomers were attributed to CB_1 and/or CB_2 receptor activation [31, 53]. Whether this is due to COX-2 or FAAH remains to be explored.

Moreover, it was suggested that some effects of *R*-flurbiprofen could be due to its bioconversion into *S*-flurbiprofen. However, we can fairly exclude the relevance of α-methylacyl-CoA racemase-dependent bioconversion of *R*-flurbiprofen into *S*-flurbiprofen [54] as the two enantiomers had, for the most part, different effects. Indeed, when given locally, strong distinct effects where observed and maintained over time for flurbiprofen enantiomers, suggesting low bioconversion in the paw tissue. Distinct effects were also observed for systemic administration, weakening the bioconversion hypothesis. Besides the potential involvement of oxygenated metabolites of endocannabinoids and the potential bioconversion of *R*-flurbiprofen into *S*-flurbiprofen, we cannot exclude an effect unrelated to COX inhibition in the effects of flurbiprofen enantiomers.

In conclusion, *R*-flurbiprofen showed anti-hyperalgesic properties in mice receiving LPS or carrageenan in the paw. However, our data suggest that the crosstalk between the endocannabinoids and prostanoids in inflammatory pain is difficult to fine tune to achieve analgesia. Moreover, COX-2 shows a complex kinetic, depending on multiple parameters, suggesting that its complete blockade does not appear to be the best solution in all settings. Our data indicate that depending on the type of nociceptive stimuli, the treatment strategy could change. Moreover, we showed that PG-Gs and PG-EAs are bioactive lipids that can modulate nociception in the LPS model of hyperalgesia. However, their exact role and effectors during the initiation and maintenance of inflammatory hyperalgesia remain to be elucidated. Nevertheless, these results underline the interest of deciphering the exact mechanism of action of both inflammatory stimuli and treatments. Indeed, depending on the origin of inflammatory pain, treatment choice and route of administration could be adapted.

Authors' contributions

B. Buisseret, M. Alhouayek and G.G. Muccioli designed research; B. Buisseret, A. Paquot, M. Alhouayek, Y. Ben Kouidar, O. Guillemot-legris and G.G. Muccioli performed experiments and analyzed data; B. Buisseret, M. Alhouayek and G.G. Muccioli wrote the paper. All authors read and approved the manuscript.

Acknowledgments :

O.G.-L. and M.A. are postdoctoral researchers from the FRS-FNRS (Fonds de la Recherche Scientifique) Belgium. G.G.M. is the recipient of subsidies from the Fonds Spéciaux de Recherches (FSR, Université catholique de Louvain) and from the FRS-FNRS, Belgium.

Conflict of interest statement:

The authors have no competing interests to declare

References

1. Sala, A.; Proschak, E.; Steinhilber, D.; Rovati, G. E., Two-pronged approach to anti-inflammatory therapy through the modulation of the arachidonic acid cascade. *Biochem Pharmacol* **2018,** *158*, 161-173.
2. Piomelli, D.; Hohmann, A. G.; Seybold, V.; Hammock, B. D., A lipid gate for the peripheral control of pain. *J Neurosci* **2014,** *34* (46), 15184-91.
3. Donvito, G.; Nass, S. R.; Wilkerson, J. L.; Curry, Z. A.; Schurman, L. D.; Kinsey, S. G.; Lichtman, A. H., The Endogenous Cannabinoid System: A Budding Source of Targets for Treating Inflammatory and Neuropathic Pain. *Neuropsychopharmacology* **2018,** *43* (1), 52-79.
4. Buisseret, B.; Alhouayek, M.; Guillemot-Legris, O.; Muccioli, G. G., Endocannabinoid and Prostanoid Crosstalk in Pain. *Trends Mol Med* **2019,** *25* (10), 882-896.
5. Woodhams, S. G.; Chapman, V.; Finn, D. P.; Hohmann, A. G.; Neugebauer, V., The cannabinoid system and pain. *Neuropharmacology* **2017,** *124*, 105-120.
6. Guindon, J.; Hohmann, A. G., The endocannabinoid system and pain. *CNS Neurol Disord Drug Targets* **2009,** *8* (6), 403-21.
7. Sasso, O.; Wagner, K.; Morisseau, C.; Inceoglu, B.; Hammock, B. D.; Piomelli, D., Peripheral FAAH and soluble epoxide hydrolase inhibitors are synergistically antinociceptive. *Pharmacol Res* **2015,** *97*, 7-15.
8. Clapper, J. R.; Henry, C. L.; Niphakis, M. J.; Knize, A. M.; Coppola, A. R.; Simon, G. M.; Ngo, N.; Herbst, R. A.; Herbst, D. M.; Reed, A. W.; Cisar, J. S.; Weber, O. D.; Viader, A.; Alexander, J. P.; Cunningham, M. L.; Jones, T. K.; Fraser, I. P.; Grice, C. A.; Ezekowitz, R. A. B.; O'Neill, G. P.; Blankman, J. L., Monoacylglycerol Lipase Inhibition in Human and Rodent Systems Supports Clinical Evaluation of Endocannabinoid Modulators. *J Pharmacol Exp Ther* **2018,** *367* (3), 494-508.
9. Kozak, K. R.; Crews, B. C.; Morrow, J. D.; Wang, L. H.; Ma, Y. H.; Weinander, R.; Jakobsson, P. J.; Marnett, L. J., Metabolism of the endocannabinoids, 2-arachidonylglycerol and anandamide, into prostaglandin, thromboxane, and prostacyclin glycerol esters and ethanolamides. *J Biol Chem* **2002,** *277* (47), 44877-85.
10. Alhouayek, M.; Muccioli, G. G., COX-2-derived endocannabinoid metabolites as novel inflammatory mediators. *Trends Pharmacol Sci* **2014,** *35* (6), 284-92.
11. Alhouayek, M.; Masquelier, J.; Cani, P. D.; Lambert, D. M.; Muccioli, G. G., Implication of the anti-inflammatory bioactive lipid prostaglandin D2-glycerol ester in the control of macrophage activation and inflammation by ABHD6. *Proc Natl Acad Sci U S A* **2013,** *110* (43), 17558-63.
12. Alhouayek, M.; Buisseret, B.; Paquot, A.; Guillemot-Legris, O.; Muccioli, G. G., The endogenous bioactive lipid prostaglandin D2-glycerol ester reduces murine colitis via DP1 and PPARgamma receptors. *FASEB J* **2018,** *32* (9), 5000-5011.
13. Buisseret, B.; Guillemot-Legris, O.; Muccioli, G. G.; Alhouayek, M., Prostaglandin D2-glycerol ester decreases carrageenan-induced inflammation and hyperalgesia in mice. *Biochim Biophys Acta Mol Cell Biol Lipids* **2019,** *1864* (5), 609-618.
14. Hu, S. S.; Bradshaw, H. B.; Chen, J. S.; Tan, B.; Walker, J. M., Prostaglandin E2 glycerol ester, an endogenous COX-2 metabolite of 2-arachidonoylglycerol, induces hyperalgesia and modulates NFkappaB activity. *Br J Pharmacol* **2008,** *153* (7), 1538-49.
15. Valdeolivas, S.; Pazos, M. R.; Bisogno, T.; Piscitelli, F.; Iannotti, F. A.; Allara, M.; Sagredo, O.; Di Marzo, V.; Fernandez-Ruiz, J., The inhibition of 2-arachidonoyl-glycerol (2-AG) biosynthesis, rather than enhancing striatal damage, protects striatal neurons from malonate-induced death: a potential role of cyclooxygenase-2-dependent metabolism of 2-AG. *Cell Death Dis* **2013,** *4*, e862.
16. Khasabova, I. A.; Uhelski, M.; Khasabov, S. G.; Gupta, K.; Seybold, V. S.; Simone, D. A., Sensitization of nociceptors by prostaglandin E2-glycerol contributes to hyperalgesia in mice with sickle cell disease. *Blood* **2019,** *133* (18), 1989-1998.
17. Gatta, L.; Piscitelli, F.; Giordano, C.; Boccella, S.; Lichtman, A.; Maione, S.; Di Marzo, V., Discovery of prostamide F2alpha and its role in inflammatory pain and dorsal horn nociceptive neuron hyperexcitability. *PLoS One* **2012,** *7* (2), e31111.
18. Hermanson, D. J.; Gamble-George, J. C.; Marnett, L. J.; Patel, S., Substrate-selective COX-2 inhibition as a novel strategy for therapeutic endocannabinoid augmentation. *Trends Pharmacol Sci* **2014,** *35* (7), 358-67.

19. Duggan, K. C.; Hermanson, D. J.; Musee, J.; Prusakiewicz, J. J.; Scheib, J. L.; Carter, B. D.; Banerjee, S.; Oates, J. A.; Marnett, L. J., (R)-Profens are substrate-selective inhibitors of endocannabinoid oxygenation by COX-2. *Nat Chem Biol* **2011,** *7* (11), 803-9.
20. Leipold, D. D.; Kantoci, D.; Murray, E. D., Jr.; Quiggle, D. D.; Wechter, W. J., Bioinversion of R-flurbiprofen to S-flurbiprofen at various dose levels in rat, mouse, and monkey. *Chirality* **2004,** *16* (6), 379-87.
21. Jamali, F.; Berry, B. W.; Tehrani, M. R.; Russell, A. S., Stereoselective pharmacokinetics of flurbiprofen in humans and rats. *J Pharm Sci* **1988,** *77* (8), 666-9.
22. Sakurada, T.; Katsumata, K.; Tan-No, K.; Sakurada, S.; Kisara, K., The capsaicin test in mice for evaluating tachykinin antagonists in the spinal cord. *Neuropharmacology* **1992,** *31* (12), 1279-85.
23. Dixon, W. J., Efficient analysis of experimental observations. *Annu Rev Pharmacol Toxicol* **1980,** *20*, 441-62.
24. Chaplan, S. R.; Bach, F. W.; Pogrel, J. W.; Chung, J. M.; Yaksh, T. L., Quantitative assessment of tactile allodynia in the rat paw. *J Neurosci Methods* **1994,** *53* (1), 55-63.
25. Edwards, S. R.; Mather, L. E.; Smith, M. T., Studies with ketamine and alfentanil following Freund's complete adjuvant-induced inflammation in rats. *Clin Exp Pharmacol Physiol* **2007,** *34* (5-6), 414-20.
26. Bottemanne, P.; Paquot, A.; Ameraoui, H.; Alhouayek, M.; Muccioli, G. G., The alpha/beta-hydrolase domain 6 inhibitor WWL70 decreases endotoxin-induced lung inflammation in mice, potential contribution of 2-arachidonoylglycerol, and lysoglycerophospholipids. *FASEB J* **2019,** *33* (6), 7635-7646.
27. Ayoub, S. S., In vitro cyclooxygenase activity assay in tissue homogenates. *Methods Mol Biol* **2010,** *644*, 117-20.
28. Kalgutkar, A. S.; Marnett, L. J., Rapid inactivation of prostaglandin endoperoxide synthases by N-(carboxyalkyl)maleimides. *Biochemistry* **1994,** *33* (29), 8625-8.
29. Booker, L.; Kinsey, S. G.; Abdullah, R. A.; Blankman, J. L.; Long, J. Z.; Ezzili, C.; Boger, D. L.; Cravatt, B. F.; Lichtman, A. H., The fatty acid amide hydrolase (FAAH) inhibitor PF-3845 acts in the nervous system to reverse LPS-induced tactile allodynia in mice. *Br J Pharmacol* **2012,** *165* (8), 2485-96.
30. Neugebauer, V.; Geisslinger, G.; Rumenapp, P.; Weiretter, F.; Szelenyi, I.; Brune, K.; Schaible, H. G., Antinociceptive effects of R(-)- and S(+)-flurbiprofen on rat spinal dorsal horn neurons rendered hyperexcitable by an acute knee joint inflammation. *J Pharmacol Exp Ther* **1995,** *275* (2), 618-28.
31. Bishay, P.; Schmidt, H.; Marian, C.; Haussler, A.; Wijnvoord, N.; Ziebell, S.; Metzner, J.; Koch, M.; Myrczek, T.; Bechmann, I.; Kuner, R.; Costigan, M.; Dehghani, F.; Geisslinger, G.; Tegeder, I., R-flurbiprofen reduces neuropathic pain in rodents by restoring endogenous cannabinoids. *PLoS One* **2010,** *5* (5), e10628.
32. Calil, I. L.; Zarpelon, A. C.; Guerrero, A. T.; Alves-Filho, J. C.; Ferreira, S. H.; Cunha, F. Q.; Cunha, T. M.; Verri, W. A., Jr., Lipopolysaccharide induces inflammatory hyperalgesia triggering a TLR4/MyD88-dependent cytokine cascade in the mice paw. *PLoS One* **2014,** *9* (3), e90013.
33. Sommer, C.; Kress, M., Recent findings on how proinflammatory cytokines cause pain: peripheral mechanisms in inflammatory and neuropathic hyperalgesia. *Neurosci Lett* **2004,** *361* (1-3), 184-7.
34. Bang, S.; Xie, Y. K.; Zhang, Z. J.; Wang, Z.; Xu, Z. Z.; Ji, R. R., GPR37 regulates macrophage phagocytosis and resolution of inflammatory pain. *J Clin Invest* **2018,** *128* (8), 3568-3582.
35. Yang, F.; Zheng, J., Understand spiciness: mechanism of TRPV1 channel activation by capsaicin. *Protein Cell* **2017,** *8* (3), 169-177.
36. Matsuda, M.; Huh, Y.; Ji, R. R., Roles of inflammation, neurogenic inflammation, and neuroinflammation in pain. *J Anesth* **2019,** *33* (1), 131-139.
37. Buritova, J.; Besson, J. M., Peripheral and/or central effects of racemic-, S(+)- and R(-)-flurbiprofen on inflammatory nociceptive processes: a c-Fos protein study in the rat spinal cord. *Br J Pharmacol* **1998,** *125* (1), 87-101.
38. Catanzaro, P. J.; Schwartz, H. J.; Graham, R. C., Jr., Spectrum and possible mechanism of carrageenan cytotoxicity. *Am J Pathol* **1971,** *64* (2), 387-404.
39. Myers, M. J.; Deaver, C. M.; Lewandowski, A. J., Molecular mechanism of action responsible for carrageenan-induced inflammatory response. *Mol Immunol* **2019,** *109*, 38-42.
40. Bennett, D. L.; Clark, A. J.; Huang, J.; Waxman, S. G.; Dib-Hajj, S. D., The Role of Voltage-Gated Sodium Channels in Pain Signaling. *Physiol Rev* **2019,** *99* (2), 1079-1151.
41. Watanabe, M.; Ueda, T.; Shibata, Y.; Kumamoto, N.; Ugawa, S., The role of TRPV1 channels in carrageenan-induced mechanical hyperalgesia in mice. *Neuroreport* **2015,** *26* (3), 173-8.

42. Diogenes, A.; Ferraz, C. C.; Akopian, A. N.; Henry, M. A.; Hargreaves, K. M., LPS sensitizes TRPV1 via activation of TLR4 in trigeminal sensory neurons. *J Dent Res* **2011,** *90* (6), 759-64.
43. Rose, T. M.; Reilly, C. A.; Deering-Rice, C. E.; Brewster, C.; Brewster, C., Inhibition of FAAH, TRPV1, and COX2 by NSAID-serotonin conjugates. *Bioorg Med Chem Lett* **2014,** *24* (24), 5695-5698.
44. Kim, S. G.; Gao, Z. G.; Soltysiak, K. A.; Chang, T. S.; Brodie, C.; Jacobson, K. A., P2Y6 nucleotide receptor activates PKC to protect 1321N1 astrocytoma cells against tumor necrosis factor-induced apoptosis. *Cell Mol Neurobiol* **2003,** *23* (3), 401-18.
45. Numazaki, M.; Tominaga, T.; Toyooka, H.; Tominaga, M., Direct phosphorylation of capsaicin receptor VR1 by protein kinase Cepsilon and identification of two target serine residues. *J Biol Chem* **2002,** *277* (16), 13375-8.
46. Vellani, V.; Mapplebeck, S.; Moriondo, A.; Davis, J. B.; McNaughton, P. A., Protein kinase C activation potentiates gating of the vanilloid receptor VR1 by capsaicin, protons, heat and anandamide. *J Physiol* **2001,** *534* (Pt 3), 813-25.
47. Chiu, I. M.; von Hehn, C. A.; Woolf, C. J., Neurogenic inflammation and the peripheral nervous system in host defense and immunopathology. *Nat Neurosci* **2012,** *15* (8), 1063-7.
48. Ansel, J. C.; Brown, J. R.; Payan, D. G.; Brown, M. A., Substance P selectively activates TNF-alpha gene expression in murine mast cells. *J Immunol* **1993,** *150* (10), 4478-85.
49. Mikami, N.; Matsushita, H.; Kato, T.; Kawasaki, R.; Sawazaki, T.; Kishimoto, T.; Ogitani, Y.; Watanabe, K.; Miyagi, Y.; Sueda, K.; Fukada, S.; Yamamoto, H.; Tsujikawa, K., Calcitonin gene-related peptide is an important regulator of cutaneous immunity: effect on dendritic cell and T cell functions. *J Immunol* **2011,** *186* (12), 6886-93.
50. Gilroy, D. W.; Colville-Nash, P. R.; Willis, D.; Chivers, J.; Paul-Clark, M. J.; Willoughby, D. A., Inducible cyclooxygenase may have anti-inflammatory properties. *Nat Med* **1999,** *5* (6), 698-701.
51. Woodhams, S. G.; Sagar, D. R.; Burston, J. J.; Chapman, V., The role of the endocannabinoid system in pain. *Handb Exp Pharmacol* **2015,** *227*, 119-43.
52. Fowler, C. J.; Janson, U.; Johnson, R. M.; Wahlstrom, G.; Stenstrom, A.; Norstrom, K.; Tiger, G., Inhibition of anandamide hydrolysis by the enantiomers of ibuprofen, ketorolac, and flurbiprofen. *Arch Biochem Biophys* **1999,** *362* (2), 191-6.
53. Ates, M.; Hamza, M.; Seidel, K.; Kotalla, C. E.; Ledent, C.; Guhring, H., Intrathecally applied flurbiprofen produces an endocannabinoid-dependent antinociception in the rat formalin test. *Eur J Neurosci* **2003,** *17* (3), 597-604.
54. de Bruin, N.; Ferreiros, N.; Schmidt, M.; Hofmann, M.; Angioni, C.; Geisslinger, G.; Parnham, M. J., Mutual inversion of flurbiprofen enantiomers in various rat and mouse strains. *Chirality* **2018,** *30* (5), 632-641.

Figure legends

Fig. 1. Systemic or local administration of flurbiprofen enantiomers decrease LPS-induced hyperalgesia.

Mice received, in 20 µL, 150 ng of LPS or saline by intra-plantar injection in the right hind paw. Mechanical hyperalgesia was monitored by an experimenter blinded to treatments using von Frey's filaments for 54 hours after LPS injection. **(A, B)** Enantiomers of flurbiprofen were administered intra-peritoneally 3 times a day. (A) Time course of mechanical hyperalgesia. The horizontal dashed line represents the mean basal 50% threshold of all groups. (B) The nociceptive score (g*h) is the basal corrected area under the curve (AUC) from the data in A. **(C, D)** Enantiomers of flurbiprofen were administered locally 30 minutes prior to LPS administration in the paw. (C) Time-course of mechanical hyperalgesia. The horizontal dashed line represents the mean basal 50% threshold of all groups. (D) The nociceptive score (g*h) is the basal corrected AUC from the data in C. Values are presented as mean ± s.e.m., n=8 animals per group. For hyperalgesia monitoring graphs (A and C): *P < 0.05 compared to the vehicle-treated LPS group, $ P < 0.05 for *S*-flurbiprofen compared to *R*-flurbiprofen treated groups, using two-way ANOVA and Holm-Sidak's multiple comparison post-hoc test. For histograms (B and D): ** P < 0.01, *** P < 0.001, compared to vehicle-treated LPS group, $$ *P* < 0.01, $$$ P < 0.001 for *S*-flurbiprofen compared to *R*-flurbiprofen treated groups, using one-way ANOVA and Dunnett's post-hoc test.

Fig. 2. Systemic or local administration of flurbiprofen enantiomers affect carrageenan-induced hyperalgesia.

Hyperalgesia was induced in mice by injection of 0.1 mg in 25 µL of carrageenan in the plantar face of the right hind paw. Mechanical hyperalgesia was monitored by an experimenter blinded to treatments using von Frey's filaments for 80 hours after carrageenan injection. **(A, B)** Enantiomers of flurbiprofen were administered intra-peritoneally 3 times a day. (A) Time course of mechanical hyperalgesia. The horizontal dashed line represents the mean basal 50% threshold of all groups. (B) The nociceptive score (g*h) is the basal corrected area under the curve (AUC) from the data in A. **(C, D)** Enantiomers of flurbiprofen were administered locally 30 minutes prior to carrageenan administration in the paw. (C) Time-course of mechanical hyperalgesia. The horizontal dashed line represents the mean basal 50% threshold of all groups. (D) The nociceptive score (g*h) is the basal corrected AUC from the data in C. Values are presented as mean ± s.e.m., n=8 animals per group. For hyperalgesia monitoring graphs (A and C): *P < 0.05, ** *P* < 0.01 compared to vehicle-treated carrageenan group, $ P < 0.05 for *S*-flurbiprofen compared to *R*-flurbiprofen treated groups, using two-way ANOVA and Holm-Sidak's multiple comparison post-hoc test. For histograms (B and D): * P < 0.05, *** P < 0.001

compared to the vehicle-treated carrageenan group, $ P < 0.05 for *S*-flurbiprofen compared to *R*-flurbiprofen treated groups using one-way ANOVA and Dunnett's post-hoc test.

Fig. 3. Expression of inflammatory cytokines in the paw of mice treated with LPS and vehicle or flurbiprofen enantiomers.

Mice received, in 20 µL, 150 ng of LPS or saline by intra-plantar injection in the right hind paw. Local injections of flurbiprofen enantiomers or vehicle were carried out 30 minutes prior to LPS injection. **(A)** mRNA expression of IL-6 and TNFα in the mice plantar tissue at 6 hours following LPS administration, measured by RT-qPCR. **(B)** IL-6 protein levels in the paw tissue measured by ELISA, at 6 hours after LPS injection. **(C)** mRNA expression of IL-6 and TNFα in the mice plantar tissue at 24 hours following LPS administration, measured by RT-qPCR. **(D)** IL-6 protein levels in the paw tissue measured by ELISA at 24 hours following LPS injection. mRNA expression is expressed relative to the control group (Veh. without LPS) set at 1. Values are presented as mean ± s.e.m., n=8 animals per group. *P < 0.05, ** P < 0.01, *** P < 0.001, compared to the vehicle-treated LPS group, using one-way ANOVA and Dunnett's post-hoc test.

Fig. 4. Expression of enzymes and immune cell markers in the paw of mice treated with and vehicle or flurbiprofen enantiomers.

Mice received, in 20 µL, 150 ng of LPS or saline by intra-plantar injection in the right hind paw. Local injections of flurbiprofen enantiomers or vehicle were carried out 30 minutes prior to LPS injection. **(A,B)** mRNA expression of COX-2, iNOS, mPGES1 and PGDS in the plantar tissue at (A) 6 hours or (B) 24 hours following LPS administration, measured by RT-qPCR. **(C, D)** mRNA expression of the pan-macrophage marker F4/80 in the plantar tissue at (C) 6 hours or (D) 24 hours following LPS administration, measured by RT-qPCR. **(E, F)** MPO activity measured in the plantar tissue at (E) 6 hours or (F) 24 hours following LPS administration. mRNA expression is expressed relative to the control group (Veh. without LPS) set at 1. Values are presented as mean ± s.e.m., n=8 animals per group. * P < 0.05, ** P < 0.01, *** P < 0.001, compared to the vehicle-treated LPS group, $ P<0.05, $$$ P<0.001, for *S*-flurbiprofen compared to *R*-flurbiprofen treated groups, using one-way ANOVA and Dunnett's post-hoc test.

Fig. 5. Local administration of flurbiprofen enantiomers at 20 hours post intra-plantar LPS worsens hyperalgesia.

Mice received, in 20 µL, 150 ng of LPS or saline by intra-plantar injection in the right hind paw. Flurbiprofen enantiomers were administered locally 20 hours after LPS administration. (A) Time-course of mechanical hyperalgesia development was monitored by a blinded experimenter using von Frey's filaments. The mean basal 50% threshold of all groups is represented by horizontal dashed line. (B) The nociceptive score (g*h) based on the area under the curve from 18 to 48 hours post LPS injection. Values are presented as mean ± s.e.m., n=8 animals per group. * $P < 0.05$, ** $P < 0.01$ *** $P < 0.001$, compared to the vehicle-treated LPS group, using two-way ANOVA for A or one-way ANOVA for B followed by Dunnett's post-hoc test.

Fig. 6. Effect of flurbiprofen enantiomers on capsaicin-induced hyperalgesia model.

Hyperalgesia was induced by intra-plantar injection of 1.6 µg of capsaicin triggering nocifensive behavior and mechanical hyperalgesia. **(A)** Nocifensive behavior is recorded for 5 minutes and measured by blinded experimenters. **(B)** Paw withdrawal threshold is determined at 1.5 hours after capsaicin injection. Values are presented as mean ± s.e.m., n=8 animals per group. * $P < 0.05$, ** $P < 0.01$, *** $P < 0.001$, compared to the vehicle-treated LPS group, using two-way ANOVA for A or one-way ANOVA for B followed by Dunnett's post-hoc test.

Fig. 7. Intra-plantar administration of prostaglandins, prostaglandin glycerol esters and prostamides affects LPS-induced hyperalgesia.

Mice received, in 20 µL, 150 ng of LPS or saline by intra-plantar injection in the right hind paw. Local injections of PG, PG-Gs, PG-EAs or vehicle were carried out 30 minutes prior to LPS injections. Mechanical hyperalgesia was monitored by an experimenter blinded to treatments using von Frey's filaments for 54 hours after LPS injection. **(A, C, E)** Time course of mechanical hyperalgesia. The horizontal dashed line represents the mean basal 50% threshold of all groups. **(B, D, F)** The nociceptive score (g*h) is the basal corrected area under the curve from the data in A, C or E, respectively. Values are presented as mean ± s.e.m., n=8 animals per group. For hyperalgesia monitoring graphs (A, C, E): * $P < 0.05$ compared to the vehicle-treated LPS group, using two-way ANOVA and Dunnett's multiple comparison post-hoc test. For histograms (B, D, F): * $P < 0.05$, ** $P < 0.01$, *** $P < 0.001$, compared to vehicle-treated LPS group, using one-way ANOVA and Dunnett's post-hoc test.

Fig. 1

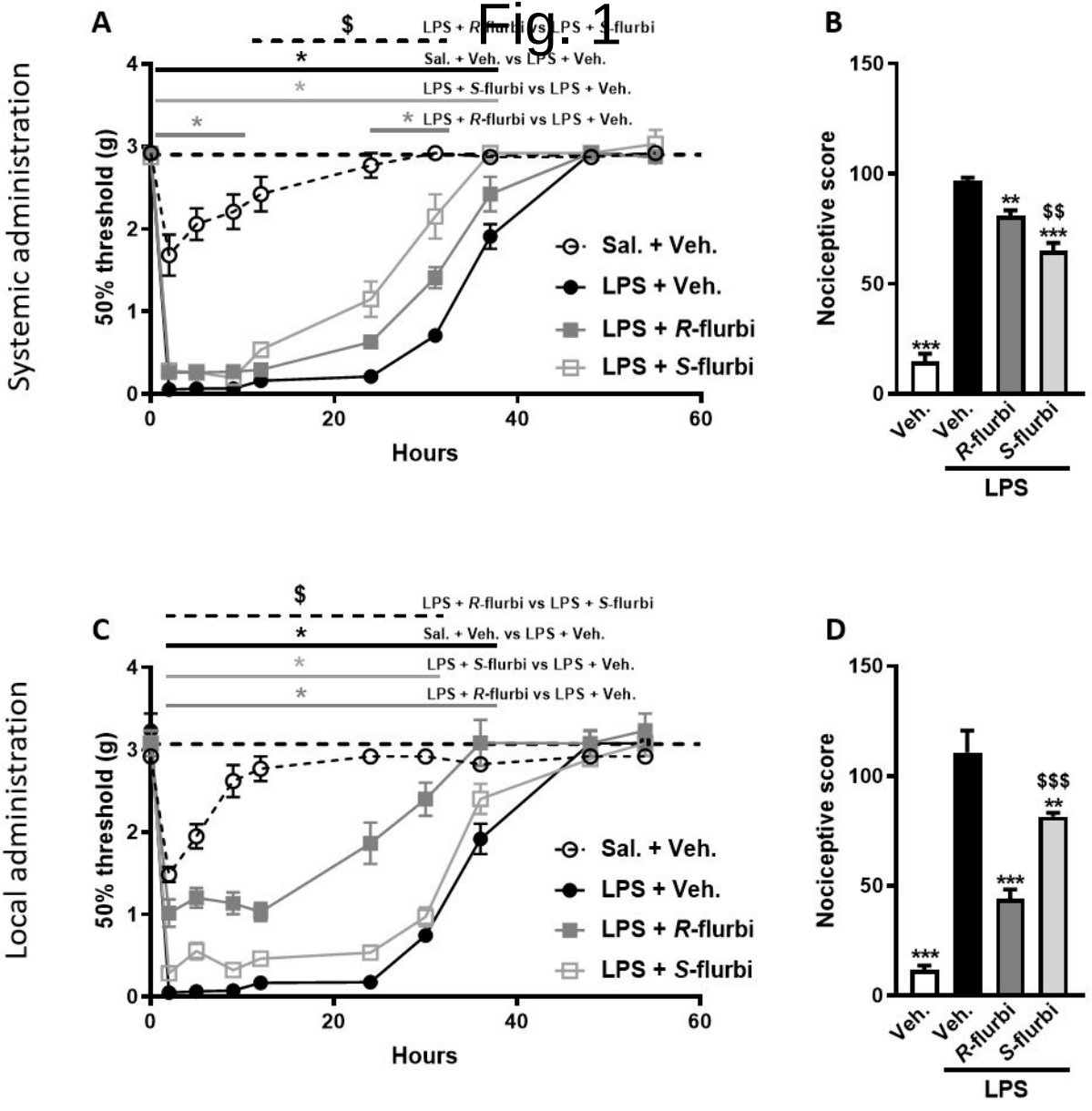
A
Systemic administration
$
LPS + R-flurbi vs LPS + S-flurbi
*
Sal. + Veh. vs LPS + Veh.
*
LPS + S-flurbi vs LPS + Veh.
*
*
LPS + R-flurbi vs LPS + Veh.
50% threshold (g)
Hours
Sal. + Veh.
LPS + Veh.
LPS + R-flurbi
LPS + S-flurbi
B
Nociceptive score
***
**
$$
***
Veh.
Veh.
R-flurbi
S-flurbi
LPS
C
Local administration
$
LPS + R-flurbi vs LPS + S-flurbi
*
Sal. + Veh. vs LPS + Veh.
*
LPS + S-flurbi vs LPS + Veh.
*
LPS + R-flurbi vs LPS + Veh.
50% threshold (g)
Hours
Sal. + Veh.
LPS + Veh.
LPS + R-flurbi
LPS + S-flurbi
D
Nociceptive score
***
***
$$$
**
Veh.
Veh.
R-flurbi
S-flurbi
LPS

Fig. 2

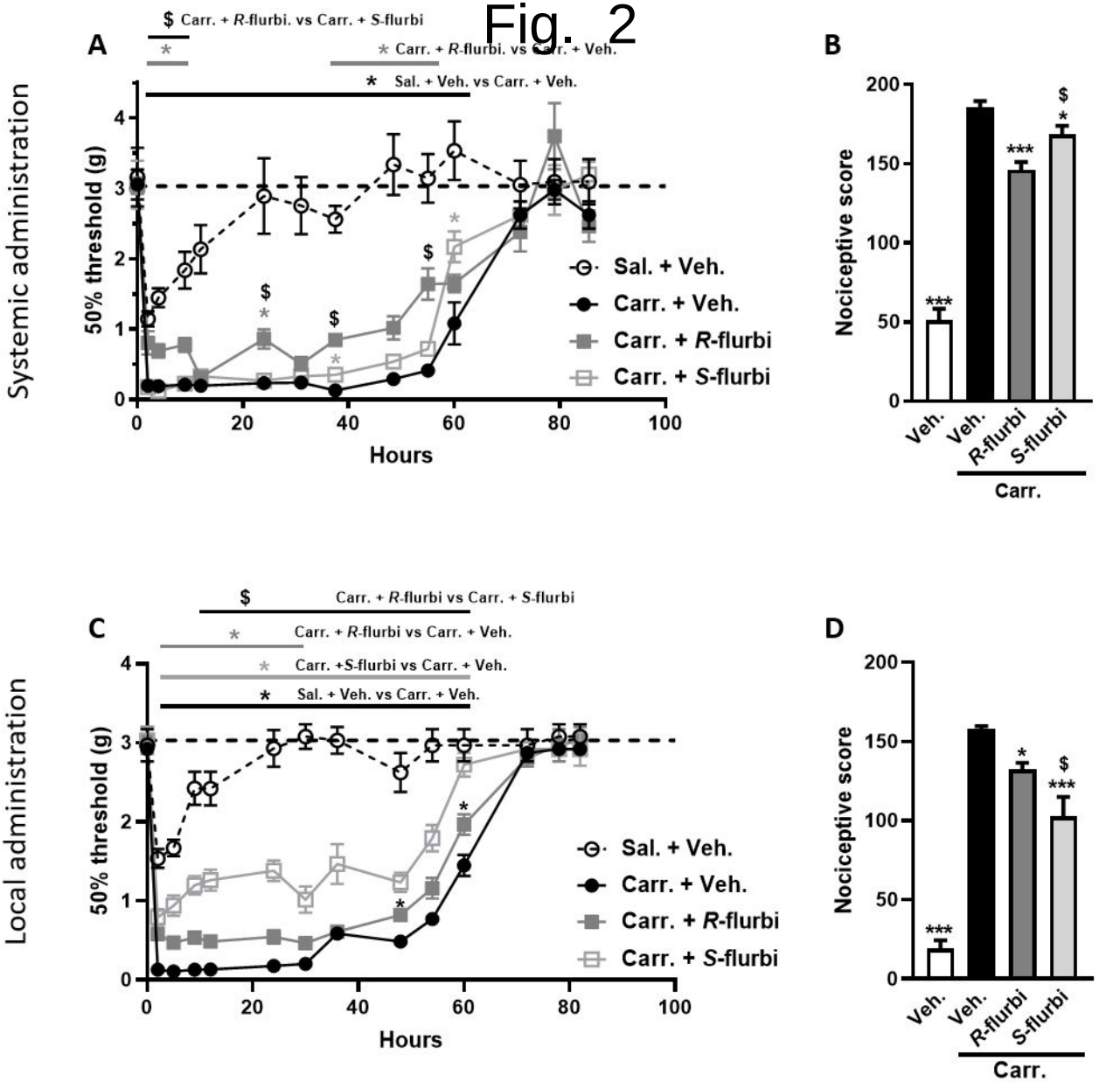
Systemic administration
A
$ Carr. + R-flurbi. vs Carr. + S-flurbi
* Carr. + R-flurbi. vs Carr. + Veh.
* Sal. + Veh. vs Carr. + Veh.
50% threshold (g)
Hours
Sal. + Veh.
Carr. + Veh.
Carr. + R-flurbi
Carr. + S-flurbi
B
Nociceptive score
Veh.
Veh.
R-flurbi
S-flurbi
Carr.
Local administration
C
$ Carr. + R-flurbi vs Carr. + S-flurbi
* Carr. + R-flurbi vs Carr. + Veh.
* Carr. +S-flurbi vs Carr. + Veh.
* Sal. + Veh. vs Carr. + Veh.
50% threshold (g)
Hours
Sal. + Veh.
Carr. + Veh.
Carr. + R-flurbi
Carr. + S-flurbi
D
Nociceptive score
Veh.
Veh.
R-flurbi
S-flurbi
Carr.

Fig. 3

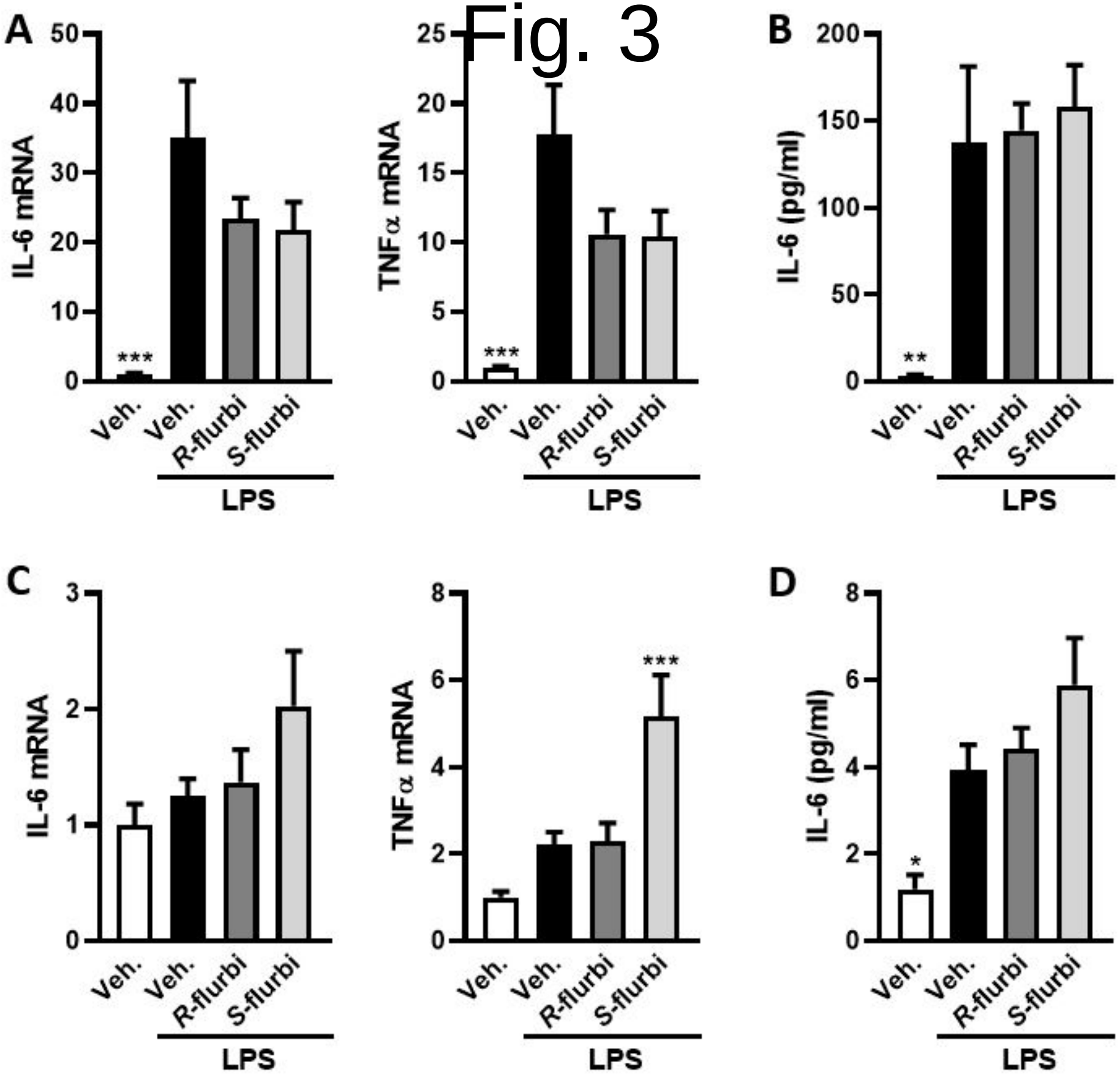
A
IL-6 mRNA
50
40
30
20
10
0
***
Veh.
Veh.
R-flurbi
S-flurbi
LPS
TNFα mRNA
25
20
15
10
5
0
***
Veh.
Veh.
R-flurbi
S-flurbi
LPS
B
IL-6 (pg/ml)
200
150
100
50
0
**
Veh.
Veh.
R-flurbi
S-flurbi
LPS
C
IL-6 mRNA
3
2
1
0
Veh.
Veh.
R-flurbi
S-flurbi
LPS
TNFα mRNA
8
6
4
2
0
***
Veh.
Veh.
R-flurbi
S-flurbi
LPS
D
IL-6 (pg/ml)
8
6
4
2
0
*
Veh.
Veh.
R-flurbi
S-flurbi
LPS

Fig. 4

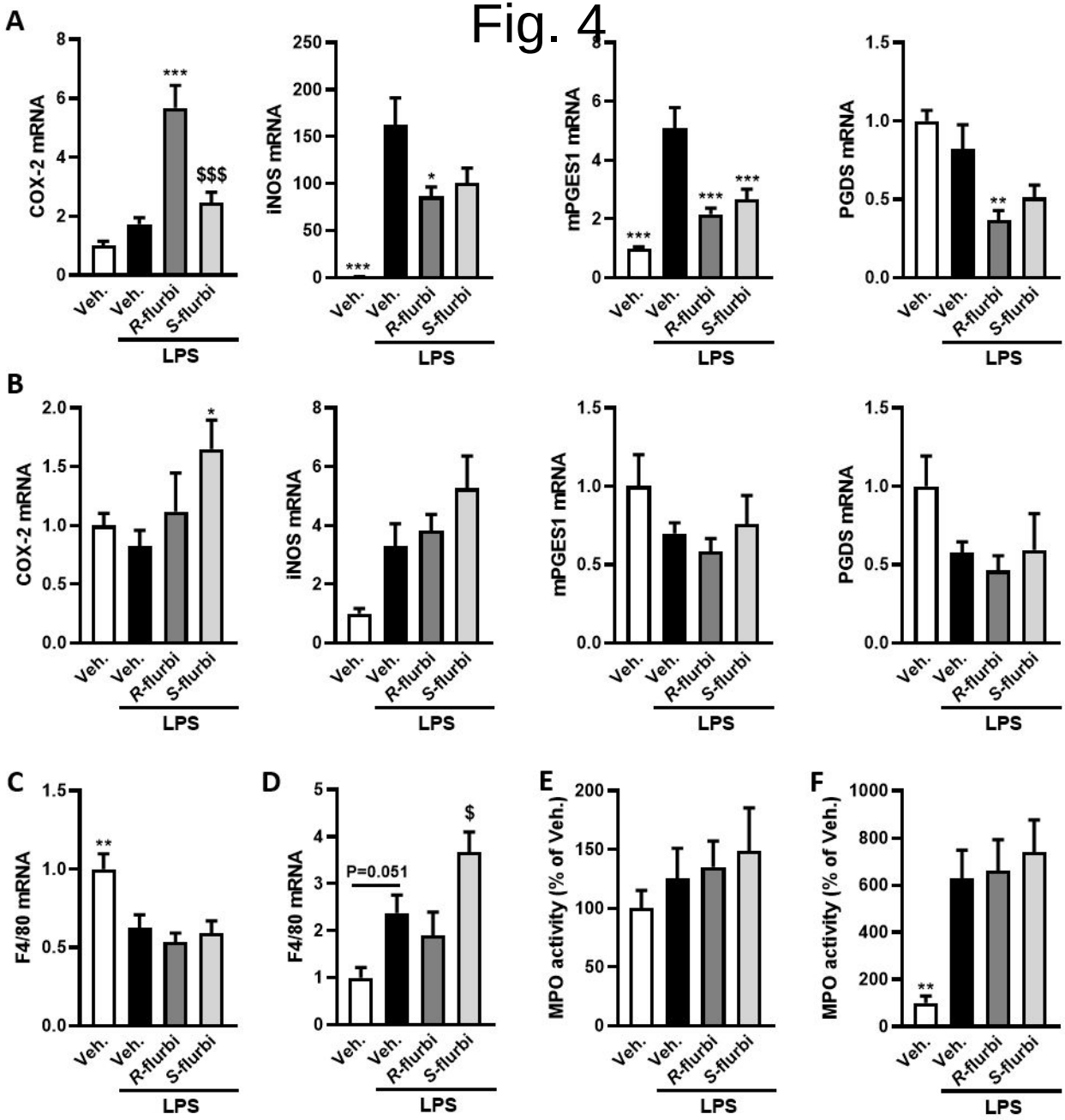
A
COX-2 mRNA
iNOS mRNA
mPGES1 mRNA
PGDS mRNA
B
COX-2 mRNA
iNOS mRNA
mPGES1 mRNA
PGDS mRNA
C
F4/80 mRNA
D
F4/80 mRNA
P=0.051
E
MPO activity (% of Veh.)
F
MPO activity (% of Veh.)
Veh.
Veh.
R-flurbi
S-flurbi
LPS

Fig. 5

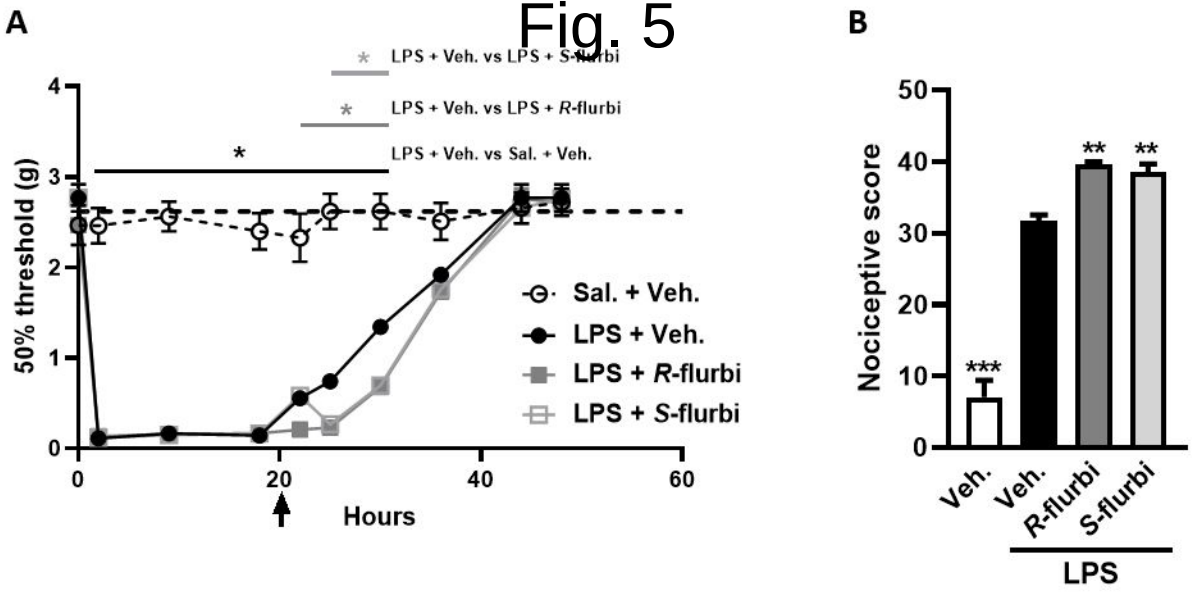
A
* LPS + Veh. vs LPS + S-flurbi
* LPS + Veh. vs LPS + R-flurbi
* LPS + Veh. vs Sal. + Veh.
50% threshold (g)
Hours
Sal. + Veh.
LPS + Veh.
LPS + R-flurbi
LPS + S-flurbi
B
Nociceptive score
***
**
**
Veh.
Veh.
R-flurbi
S-flurbi
LPS

Fig. 6

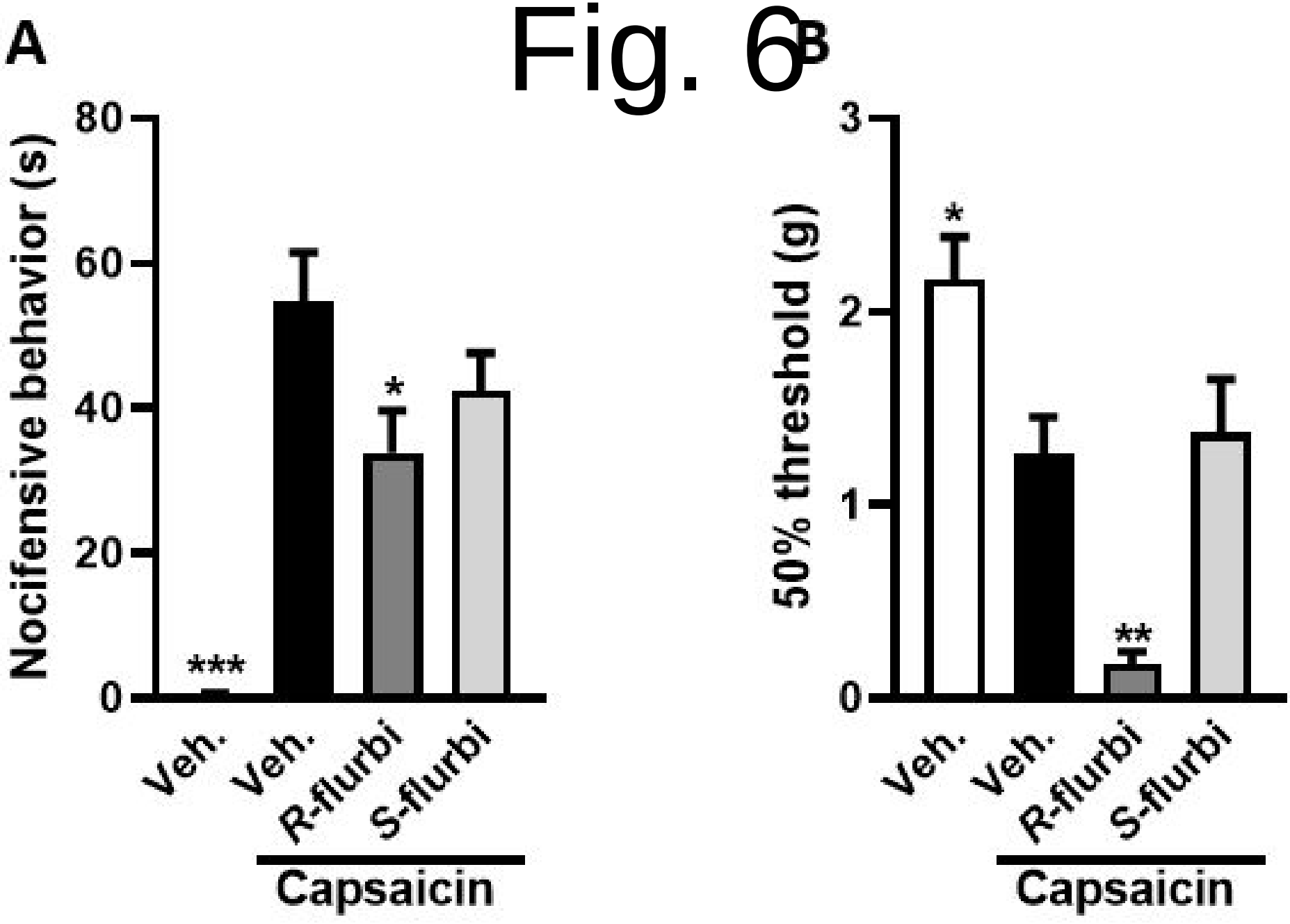
A
Nocifensive behavior (s)
80
60
40
20
0
***
*
Veh.
Veh.
R-flurbi
S-flurbi
Capsaicin
B
50% threshold (g)
3
2
1
0
*
**
Veh.
Veh.
R-flurbi
S-flurbi
Capsaicin

Fig. 7

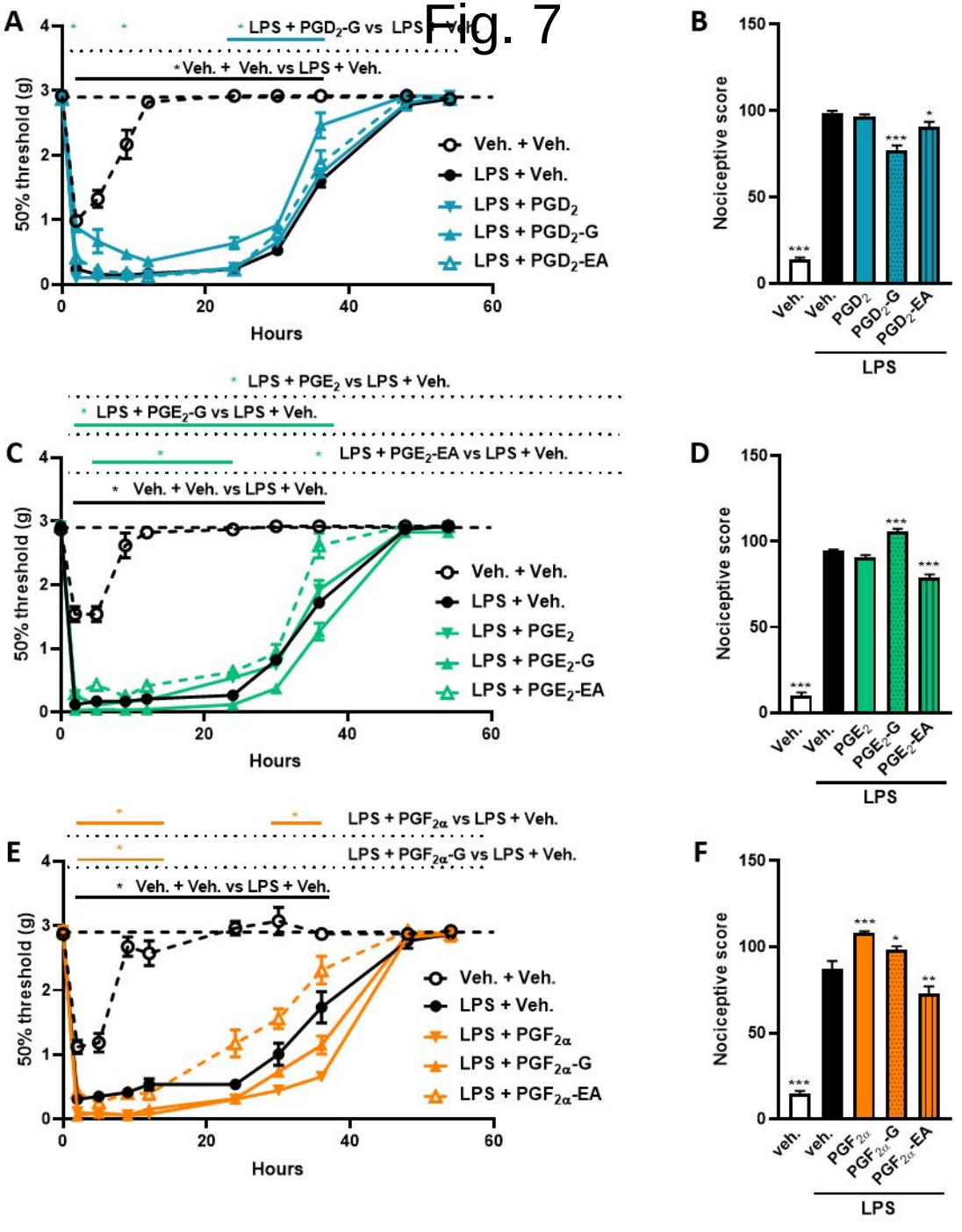
A
* LPS + PGD2-G vs LPS + Veh.
*Veh. + Veh. vs LPS + Veh.
50% threshold (g)
Hours
Veh. + Veh.
LPS + Veh.
LPS + PGD2
LPS + PGD2-G
LPS + PGD2-EA
B
Nociceptive score
Veh.
Veh.
PGD2
PGD2-G
PGD2-EA
LPS
* LPS + PGE2 vs LPS + Veh.
* LPS + PGE2-G vs LPS + Veh.
C
* LPS + PGE2-EA vs LPS + Veh.
* Veh. + Veh. vs LPS + Veh.
50% threshold (g)
Hours
Veh. + Veh.
LPS + Veh.
LPS + PGE2
LPS + PGE2-G
LPS + PGE2-EA
D
Nociceptive score
Veh.
Veh.
PGE2
PGE2-G
PGE2-EA
LPS
* LPS + PGF2α vs LPS + Veh.
* LPS + PGF2α-G vs LPS + Veh.
E
* Veh. + Veh. vs LPS + Veh.
50% threshold (g)
Hours
Veh. + Veh.
LPS + Veh.
LPS + PGF2α
LPS + PGF2α-G
LPS + PGF2α-EA
F
Nociceptive score
veh.
veh.
PGF2α
PGF2α-G
PGF2α-EA
LPS

Fig.S1

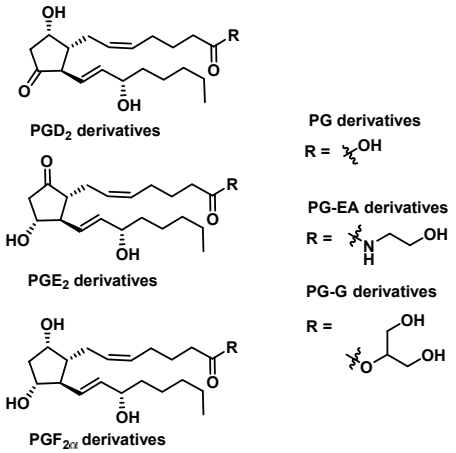

Fig. S1. Structure of COX-2 derived endocannabinoid metabolites and of the flurbiprofen enantiomers.
(A) Structure of the prostaglandins PGD_2, PGE_2 and $PGF_{2\alpha}$, and of the corresponding ethanolamide (PG-EA) and glycerol ester (PG-G) derivatives. The key for the R substituent is shown on the right. **(B)** Structures of the enantiomers of flurbiprofen.

Fig.S2

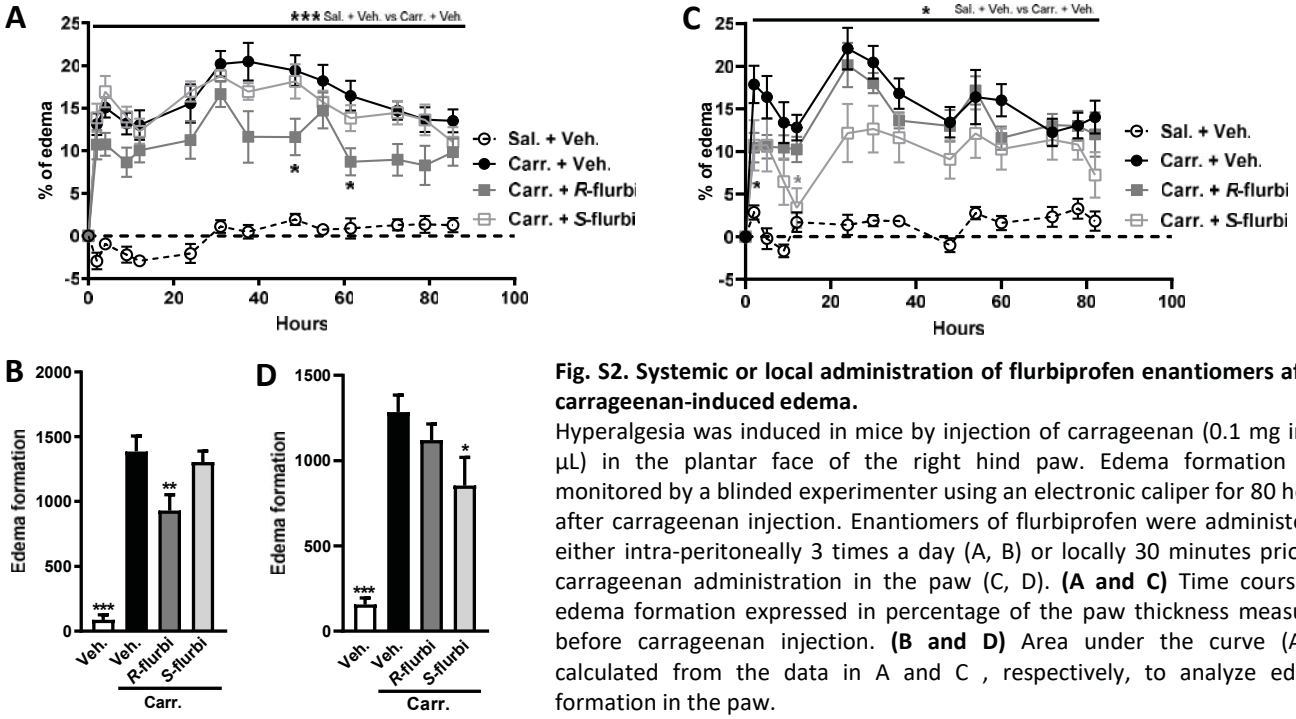

Fig. S2. Systemic or local administration of flurbiprofen enantiomers affect carrageenan-induced edema.
Hyperalgesia was induced in mice by injection of carrageenan (0.1 mg in 25 µL) in the plantar face of the right hind paw. Edema formation was monitored by a blinded experimenter using an electronic caliper for 80 hours after carrageenan injection. Enantiomers of flurbiprofen were administered either intra-peritoneally 3 times a day (A, B) or locally 30 minutes prior to carrageenan administration in the paw (C, D). **(A and C)** Time course of edema formation expressed in percentage of the paw thickness measured before carrageenan injection. **(B and D)** Area under the curve (AUC) calculated from the data in A and C , respectively, to analyze edema formation in the paw.
Values are mean ± s.e.m., n=8 animals per group. For edema formation monitoring graphs (A and C): *P < 0.05, *** *P* < 0.001 compared to vehicle-treated carrageenan group using two-way ANOVA and Holm-Sidak's multiple comparison post-hoc test. For histograms (B and D): * P < 0.05, ** P < 0.01 , *** P < 0.001 compared to vehicle-treated carrageenan group, using one-way ANOVA and Dunnett's post-hoc test.

Fig.S3

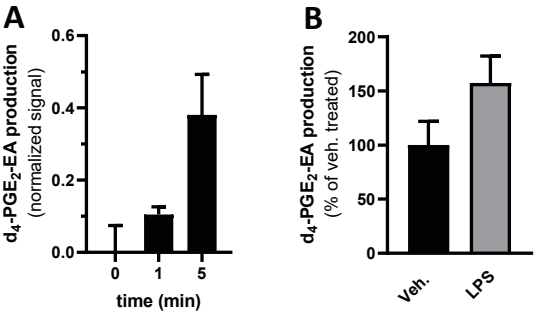

Fig. S3. d_4-PGE_2-EA production in paw homogenates.
(**A**) Mice paw tissue homogenates were incubated in the presence of d_4-AEA (10µM) for 1 or 5 min. After quenching of the reaction with cold methanol and addition of an internal standard, the lipids were extracted and analyzed by UPLC-MS/MS. The signal obtained for samples from d_4-AEA incubated in the same homogenates in the presence of methanol (0 in the graph) was subtracted to take into account potential non-enzymatic production of d_4-PGE_2-EA. (**B**) Paw tissue homogenates from mice that received an intra-plantar injection of saline or LPS (20 µL, 150 ng) for 2hours were incubated in the presence of d_4-AEA (10µM, 5min). Samples were then analyzed as in (A). For the tissue homogenate of each mouse, a similar incubation was performed in the presence of methanol and the signal subtracted as described in (A). Values are mean ± s.e.m., n=5 animals per group.